

ČESKÉ VYSOKÉ UČENÍ TECHNICKÉ V PRAZE

Fakulta stavební

Katedra betonových a zděných konstrukcí



Studijní program: Integrovaná bezpečnost staveb

Diplomová práce

**ANALÝZA BETONOVÝCH KONSTRUKCÍ VYSTAVENÝCH
MECHANICKÉMU A TEPLŮTNÍMU ZATÍŽENÍ**

**ANALYSIS OF CONCRETE STRUCTURES EXPOSED TO
MECHANICAL AND THERMAL LOADING**

Autor práce: Bc. Alžběta Kohoutová

Vedoucí práce: Ing. Radek Štefan, Ph.D., FEng.

Praha 2022

ZADÁNÍ DIPLOMOVÉ PRÁCE

I. OSOBNÍ A STUDIJNÍ ÚDAJE

Příjmení: Kohoutová Jméno: Alžběta Osobní číslo: 468376
 Zadávací katedra: K133 - Katedra betonových a zděných konstrukcí
 Studijní program: Stavební inženýrství
 Studijní obor: Integrální bezpečnost staveb

II. ÚDAJE K DIPLOMOVÉ PRÁCI

Název diplomové práce: Analýza betonových konstrukcí vystavených mechanickému a teplotnímu zatížení
 Název diplomové práce anglicky: Analysis of concrete structures exposed to mechanical and thermal loading

Pokyny pro vypracování:
 Rešerše literatury
 Příklady konstrukcí
 Výpočetní modely a metody
 Výpočty
 Vyhodnocení
 Závěr

Seznam doporučené literatury:

ZIENKIEWICZ, Olek C., TAYLOR, Robert L. a ZHU, J. Z. The Finite Element Method: Its Basis and Fundamentals. 6th ed. Oxford: Elsevier Butterworth-Heinemann, 2005. ISBN 9780080472775.

KIM, Nam-Ho. Introduction to Nonlinear Finite Element Analysis. New York: Springer US, 2015. ISBN 978-1-4419-1746-1.

ŠTEFAN, R. Transport Processes in Concrete at High Temperatures. Mathematical Modelling and Engineering Applications with Focus on Concrete Spalling. PhD thesis, CTU in Prague, 2015.

Jméno vedoucího diplomové práce: Ing. Radek Štefan Ph.D.

Datum zadání diplomové práce: 29.9.2021 Termín odevzdání DP v IS KOS: 2.1.2022
Údaj uveďte v souladu s datem v časovém plánu příslušného ak. roku

Podpis vedoucího práce

Podpis vedoucího katedry

III. PŘEVZETÍ ZADÁNÍ

Beru na vědomí, že jsem povinen vypracovat diplomovou práci samostatně, bez cizí pomoci, s výjimkou poskytnutých konzultací. Seznam použité literatury, jiných pramenů a jmen konzultantů je nutné uvést v diplomové práci a při citování postupovat v souladu s metodickou příručkou ČVUT „Jak psát vysokoškolské závěrečné práce“ a metodickým pokynem ČVUT „O dodržování etických principů při přípravě vysokoškolských závěrečných prací“.

Datum převzetí zadání

Podpis studenta(ky)

Čestné prohlášení

Prohlašuji, že jsem diplomovou práci na téma „Analýza betonových konstrukcí vystavených mechanickému a teplotnímu zatížení“ vypracovala samostatně pod vedením Ing. Radka Štefana, Ph.D., FEng. a že jsem uvedla veškeré použité informační zdroje v souladu s Metodickým pokynem o dodržování etických principů při přípravě vysokoškolských závěrečných prací.

V Praze dne 1. 1. 2022

.....

Alžběta Kohoutová

Poděkování

Děkuji panu Ing. Radku Štefanovi, Ph.D, FEng, za odborné vedení mé diplomové práce, za ochotu, cenné rady a připomínky, které pro mě byly velmi přínosné, a bez kterých by tato práce nevznikla. Děkuji rovněž paní Mgr. Yuliii Khmurovske, Ph.D. za konzultace, které mi pomohly s vypracováním kapitol 5.1 a 5.2 této práce. V neposlední řadě touto formou děkuji své rodině za podporu při studiu.

Tato diplomová práce byla vytvořena v rámci projektu Studentské grantové soutěže ČVUT, č. projektu SGS21/040/OHK1/1T/11.

Abstrakt

Hlavní náplní této práce je vytvoření algoritmu pro analýzu železobetonové stropní desky vystavené teplotnímu zatížení. Deska je posuzována metodou založenou na závislosti momentu a křivosti.

Obsah této práce je formálně rozdělen do dvou částí. V první části jsou teoreticky i prakticky popsány mechanické a teplotní výpočty, které ukazují možnosti analýzy různých typů konstrukcí vystavených mechanickému či teplotnímu zatížení. Rovněž jsou v této části popsány metody posuzování konstrukcí za požáru, z nichž některé byly použity k ověření správnosti vytvořeného algoritmu. Druhá část práce se věnuje komplexní mechanické a teplotní analýze stropní konstrukce v podobě algoritmu, který je v této části detailně popsán. Rovněž je zde vysvětlen způsob, jakým se ubíral vývoj zmíněného algoritmu.

Klíčová slova

železobetonová deska; mechanická analýza; teplotní analýza; numerická analýza; metoda moment-křivost; požár; požární odolnost; metoda konečných prvků

Abstract

The main aim of this thesis is designing an algorithm for an analysis of a reinforced concrete ceiling slab which is exposed to thermal loading. The analysis is based on a moment-curvature approach.

The content of this work is formally divided into two parts. In the first part the structural and thermal calculations are theoretically and practically explained with the use of several illustrative examples. The methods for analyzing structures exposed to fire are described in this part, some of which are later used to provide a verification of the designed algorithm. The second part covers the complex mechanical and thermal analysis of the ceiling slab which takes form of an algorithm, the principle of which is closely explained in this part as well, together with the approach to the development of this algorithm.

Keywords

reinforced concrete slab; mechanical analysis; thermal analysis; numerical analysis; moment-curvature approach; fire; fire resistance; finite element method

Contents

List of figures	9
1 Introduction	12
1.1 Motivation and goals.....	12
2 Methods of analysis of structures	14
2.1 Mechanical analysis	14
2.2 Thermal analysis	15
3 Methods of analysis of concrete structures at high temperatures	16
3.1 The usage of tabulated data.....	16
3.2 Simplified calculation methods.....	17
3.2.1 500°C isotherm method	17
3.2.2 Zone method	20
3.2.3 Method for columns based on a curvature estimate	22
4 Finite Element Method	23
4.1 Introduction to Finite Element Method.....	23
4.2 Principle of Finite Element Method.....	23
4.3 Finite Element Method in Thermal Analysis.....	24
4.3.1 Mesh	24
4.3.2 Material parameters	25
4.3.3 Boundary conditions	25
4.3.4 Thermal analysis of the structure.....	26
4.3.5 Conclusion	27
5 Mechanical Analysis	28
5.1 Structural Element	28
5.1.1 Assembly and analysis of the structure.....	29
5.1.2 Boundary conditions	30
5.1.3 Conclusion	31
5.2 Nonlinear mechanical analysis	32
5.2.1 Assembly	33
5.2.2 Boundary conditions.....	33
5.2.3 Analysis of a nonlinear structure	33
5.2.4 Conclusion	36
5.3 Direct Stiffness Method in truss mechanical analysis	37
5.3.1 Mechanical analysis – prescribed force	38
5.3.2 Mechanical analysis – prescribed force, reactions.....	39
5.3.3 Mechanical analysis – prescribed displacement, reactions.....	42
5.3.4 Mechanical analysis – prescribed force and thermal loading	44
5.3.5 Axial forces and deformation – force loading	45
5.3.6 Axial forces and deformation – force and thermal loading	46
5.3.7 Complex example	49
6 Analysis of a reinforced concrete ceiling slab at normal temperature.....	53
6.1 Required inputs	55

6.1.1	Material properties at normal temperature.....	55
6.2	Load-bearing capacity at normal temperature	56
6.2.1	Forces in reinforcements.....	56
6.2.2	Forces in concrete	57
6.2.3	The load-bearing capacity.....	57
6.3	Methods of determining the height of the compressed part of the cross-section.....	58
6.4	The description of the algorithm at normal temperature	60
6.5	Verification with existing programs	62
6.5.1	Benchmark example No. 1.....	62
6.5.2	Benchmark example No. 2.....	66
6.5.3	Benchmark example No. 3.....	69
6.5.4	Assessment	71
7	Analysis of a reinforced concrete ceiling slab at high temperature.....	72
7.1	Temperatures in the structure.....	73
7.2	Load-bearing capacity at high temperatures	76
7.2.1	Material properties at high temperature.....	76
7.2.2	Strain.....	79
7.2.3	The description of the algorithm at high temperature.....	81
7.2.4	The effect of high temperatures on load-bearing capacity	85
7.3	Verification with existing methods	86
7.3.1	Benchmark example No. 1.....	86
7.3.2	Benchmark example No. 2.....	89
7.3.3	Benchmark example No. 3.....	92
7.3.4	Assessment	95
8	Conclusion.....	96
Literature	97
Software	99

List of figures

Figure 1 Temperature profile (generated from [1]).....	18
Figure 2 Coefficient $ks\theta$ allowing for decrease of characteristic strength f_{yk} (taken from [6])	19
Figure 3 Cross-section division (taken from [11]).....	20
Figure 4 Coefficient $kc\theta$ allowing for decrease of characteristic strength f_{ck} (taken from [6])	21
Figure 5 Determination of first order moment capacity $MORd, fi$ (taken from [6])	22
Figure 6 Mesh (created in [16]).....	25
Figure 7 Material parameters assigned to reinforced concrete (A) and floor layer (B)	25
Figure 9 Function of the heat flux.....	26
Figure 10 Temperature distribution in the cross-section at $t = 30$ min (created in [17])	27
Figure 11 Truss structure subjected to mechanical loading.....	28
Figure 12 Numbers assigned to elements and nodes.....	29
Figure 13 Serially connected nonlinear springs (taken from [10])	32
Figure 14 Results obtained using Newton method	35
Figure 15 Results obtained using modified Newton method	35
Figure 16 Official results (taken from [10])	35
Figure 17 Truss structure (created in [17])	37
Figure 18 Element numbers and force in node 4 (taken from [12])	38
Figure 19 Code numbers (taken from [12])	38
Figure 20 Example with prescribed force	40
Figure 21 Split of stiffness matrix.....	41
Figure 22 Example with prescribed displacement.....	42
Figure 23 Example with prescribed force and thermal loading.....	44
Figure 24 Truss example (taken from [14]).....	47
Figure 25 Truss example (created in [1]).....	47
Figure 26 Truss structure.....	49
Figure 27 Truss structure (created in MATLAB)	49
Figure 28 Displacements and axial forces.....	51
Figure 29 Displacements and axial forces after raising the temperature in the lower bars.....	52
Figure 30 Displacements and axial forces without thermal loading	52
Figure 31 Moment-curvature diagram (taken from [8])	53
Figure 32 Parabolic-rectangular stress-strain diagram of concrete (taken from [7]).....	55

Figure 33 Bi-linear stress-strain diagram of steel (taken from [7])	56
Figure 34 Input in the designed algorithm	62
Figure 35 Output from the designed algorithm; moment-curvature diagram.....	63
Figure 36 RCC [19] Preprocessor	64
Figure 37 RCC [19] Postprocessor.....	64
Figure 38 Input in InDion [20]	65
Figure 39 Output from InDion [20].....	65
Figure 40 Input in the designed algorithm	66
Figure 41 Output from the designed algorithm; moment-curvature diagram.....	66
Figure 42 RCC [19] Preprocessor	67
Figure 43 RCC [19] Postprocessor.....	67
Figure 44 Input in InDion [20]	68
Figure 45 Output from InDion [20].....	68
Figure 46 Input in the designed algorithm.....	69
Figure 47 Output from the designed algorithm; moment-curvature diagram.....	69
Figure 48 Input in InDion [20]	70
Figure 49 Output from InDion [20].....	70
Figure 50 Complete temperature data (obtained from [17])	73
Figure 51 TempAnalysis preprocessor	74
Figure 52 Values used for interpolation	74
Figure 53 Temperature profile at $t = 60$ min (generated from [1]).....	75
Figure 54 Input in the algorithm for linear interpolation	75
Figure 55 Stress-strain diagram of concrete at high temperatures (taken from [6])	76
Figure 56 Values for the parameters of the stress-strain relationship of concrete (taken from [6]).....	77
Figure 57 Stress-strain diagram of steel at high temperatures (taken from [6])	78
Figure 58 Values for the parameters of the stress-strain relationship of steel (taken from [6])	78
Figure 59 Total thermal elongation of concrete (taken from [6])	79
Figure 60 Total thermal elongation of steel (taken from [6])	80
Figure 61 Illustration of the thermal strain effect on the output (created in [18])	81
Figure 62 Temperature development at $x = 30$ mm (generated from [16]).....	85
Figure 63 Comparison of moment-curvature diagrams for different times (created in [18]).	86
Figure 64 TempAnalysis [17] preprocessor.....	87
Figure 65 Input in the designed algorithm.....	87

Figure 66 Output from the designed algorithm; moment-curvature diagram.....	88
Figure 67 Temperature profile at $t = 60$ min (generated from [16])	88
Figure 68 TempAnalysis [17] preprocessor.....	90
Figure 69 Input in the designed algorithm.....	90
Figure 70 Output from the designed algorithm; moment-curvature diagram.....	91
Figure 71 Temperature profile at $t = 75$ min (generated from [17])	91
Figure 72 TempAnalysis [17] preprocessor.....	93
Figure 73 Input in the designed algorithm.....	93
Figure 74 Output from the designed algorithm; moment-curvature diagram.....	94
Figure 75 Temperature profile at $t = 75$ min (generated from [17])	94

1 Introduction

1.1 Motivation and goals

Thermal and mechanical analyses of reinforced concrete structures are a crucial part of structural design. There are many approaches from handwritten simplified equations to complex models which take advantage of advanced computational software. The analyzed projects themselves cover a wide range as well, from simply supported elements to compound structures. It is a job of a structural designer to determine which element or structure needs to be analyzed using which method.

However, structural designers and especially fire protection designers very often need to analyze simple structural elements, such as columns, beams, walls, or slabs, to determine their load-bearing capacity, either at normal or at high temperatures. For that, computational algorithms designed by the Department of Concrete and Masonry Structures at the Faculty of Civil Engineering are widely used amongst professionals as well as students of the Faculty of Civil Engineering, due to their user-friendly environment, short calculating time, precision, and the ability to run on standard computational devices.

The Department of Concrete and Masonry Structures at the Faculty of Civil Engineering has already developed many algorithms which come very handy during thermal and mechanical analyses of reinforced concrete structures both at normal and high temperatures. However, there are topics yet to be covered, especially regarding the mechanical analysis at high temperatures. Specifically, there is no algorithm which determines the load-bearing capacity of a reinforced concrete ceiling slab exposed to high temperatures. Therefore, the goal of this thesis is to design such algorithm to help simplify and speed up the structural design.

This work is a result of two consecutive semester courses, 124SEM and 133DPM. I started the first of these two semesters having no experience with advanced numerical analyses of structures, therefore my main aim was to get an overview of how to analyze firstly mechanical and consequently thermal behavior of structures. I focused on mechanical and thermal analyses separately through smaller examples, which allowed me to go into more detail. In the second semester we decided to couple the thermal and mechanical analyses into one algorithm, which would deal with both thermal and mechanical behavior of a specific structural element with variable material properties and geometry. As this led to a complex investigation of structures at high temperatures, which would need more than one semester to completely cover

and therefore would exceed the diploma thesis range, we decided to simplify both thermal and mechanical analyses in the algorithm compared to the separate examples.

This gradual development is one of the reasons why this thesis consists of two parts. The first part introduces numerical thermal analysis and shows various ways of analyzing mechanical behavior of structures. Moreover, the first part holds a general overview of various approaches used in thermal and mechanical analyses together with selected practical examples which led to the algorithm itself.

The second part focuses on creating an algorithm, which investigates a reinforced concrete ceiling slab exposed to high temperatures. There are many possible approaches to cover the analysis of this slab (e.g., [1]), some of which are introduced amongst the separate thermal and mechanical analyses in the first part of this work. Eventually, we decided to go with a numerical method, which takes advantage of the moment-curvature dependency, for it is quite straightforward, possible to code in a span of one semester and very accurate. The basis of the analysis of the reinforced concrete ceiling slab lies in the moment-curvature approach, which is covered e.g., in [2] or in [3]. Even though most of the procedures shown in the first part of this work do not occur in the final algorithm, they provide a better insight in the possible ways of studying thermal and mechanical behavior of different types of structures. Therefore, I consider them an asset and resource which helped me to a better understanding of the given matters, which is also why I included them in this work.

The main goals of this work are:

- 1) Design of an algorithm, which determines the load-bearing capacity of a reinforced concrete ceiling slab exposed to high temperatures.
- 2) Comparison of the results obtained from the program executing the algorithm with results from other methods and existing programs.

2 Methods of analysis of structures

2.1 Mechanical analysis

Mechanical analysis is a process of searching for a reaction of a structure to a prescribed loading. When analyzing a structure, boundary conditions such as geometry and material properties as well as the support system and type, size, and position of loading need to be defined. The purpose of a mechanical analysis is usually to find unknown displacements and deformations, reactions, internal forces, and stresses [4].

Individual elements as well as whole structures can be analyzed, whereas the applied methods change with the size and complexity of the analyzed subject and desired accuracy [5].

There are many methods and theories which are implemented when analyzing structures. Among them count theoretical analytical models or numerical methods. Former are used for accurate determination of deformation and stress in elements using differential and integral equations. This solution is called the *accurate problem solution*. Latter define how to numerically approximate mathematical problems by imposing simplifying assumptions. By implementing these assumptions complicated equations are simplified, so they can be solved numerically with use of computational software. Since the original equations are not accurately solved, it is called *approximate problem solution* [4].

Amongst numerical methods used for not only mechanical but for thermal analysis as well, count for example Finite Element Method (FEM), which discretizes continuum into finite number of elements. Another one is Finite Difference Method, which approximates derivations in differential equation by differences, changing differential equations into difference equations [5].

2.2 Thermal analysis

Thermal analysis is a process of determining the temperatures of the structure when exposed to high temperatures, most commonly a fire. The actual fire is during the analysis replaced by a fire model. The fire models are divided into two main groups:

- Nominal fire curves according to EN 1991-1-2 [6]
 - amongst nominal fire curves counts for example the standard fire curve ISO 834 defined in EN 1991-1-2 [6],
 - those fire curve do not include the cooling phase.
- Natural fire models
 - simplified fire models, such as the parametric curve defined in EN 1991-1-2 [6],
 - advanced fire models such as the zone models or CFD models,
 - these models include the cooling phase.

In the solved examples introduced in the next chapters, the development of high temperatures follows the ISO 834 curve defined in EN 1991-1-2 [6]. This fire model was selected for this work due to its widest range of usage, compatibility with standards, simplicity, and conservative results.

The main part of the thermal analysis is a heat transfer between the environment and the structure. There are several approaches to model the heat transfer from simple but inaccurate to highly complex ones. In the examples solved in this work, the thermal analysis is carried out using the Finite Element Method, which very accurately simulates the real heat transfer ([1]). Another reason for choosing the finite element method for the thermal analysis is its potential to obtain results with the use of standard computational devices. The number of elements which the structure is divided into, and therefore the precision of obtained results, can be customized to fit the capacity of the computational device in use, with the obvious positive or negative impact on the precision of the method.

3 Methods of analysis of concrete structures at high temperatures

There are several methods which might be implemented when analyzing concrete structures at high temperatures. This chapter briefly describes especially those used for a ceiling slab analysis. Possible methods are described in detail in EN 1992-1-2 [7].

According to EN 1992-1-2 [7], there are several possible approaches to determine the fire resistance of a concrete structure. Those are:

- normalized tests of fire resistance,
- usage of tabulated data,
- design with use of simplified calculation methods,
- design with use of advanced calculation methods,
- full-scale testing.

The factors which determine the approach used for given design are the type of structure, the purpose of the building, required accuracy, computational devices at hand, used materials, time allowed to obtain results and other.

3.1 The usage of tabulated data

Tabulated data obtained from former repeated experiments and calculations and included in the standards are in many cases the easiest and fastest way to determine the fire resistance of a structural element.

However, some restrictions exist as to when the tabulated data can be used.

- Tabulated data are determined from experiments and calculations, where the fire is represented by the nominal fire curve ISO 834 defined in EN 1991-1-2 [6]. Therefore, these values cannot be used for any other fire model.
- Tabulated data included in EN 1992-1-2 [7] exist only for certain structural elements, such as
 - columns,
 - walls,
 - tensile members,
 - beams,
 - slabs.

The usage of tabulated data is very conservative. That is why this approach usually serves as a pre-design, to obtain a general ideal of the fire resistance of a given

structure. If the analyzed structure does not meet the required fire resistance with the use of tabulated data, it is necessary to choose a more accurate way of the fire resistance determination, such as one of the simplified calculation methods.

3.2 Simplified calculation methods

These methods are the most accurate ways of analyzing concrete structures without the use of complex computer software. The main advantage of these methods is that most of the calculations can be done by hand while still maintaining a reasonable accuracy.

Amongst the simple computational methods according to EN 1992-1-2 [7] count

- 500°C isotherm method for members subjected to the bending moment, and/or the normal force,
- zone method for members subjected to the bending moment, and/or the normal force,
- method for columns based on a curvature estimate,
- method for verification of the load-bearing capacity in shear and torsion,
- simplified calculation method for beams and slabs.

When it comes to analyzing a reinforced concrete slab, which is an element subjected to a bending moment, the 500°C isotherm and the zone methods are commonly used. Both methods are explained in detail in EN 1992-1-2 [7], however, general overviews of both methods are given in the next subchapters. The method for columns based on a curvature estimate is briefly described as well, as it forms the basis of the procedure implemented in the designed algorithm.

3.2.1 500°C isotherm method

This method is based on following assumptions:

- structure is subjected to standard fire curve ISO 834 or parametric fire curve,
- concrete of a temperature under 500°C keeps all its material properties including the strength same as at normal temperatures,
- concrete of a temperature above 500°C loses its strength completely, therefore it is neglected, resulting in the reduction of the cross-section dimensions,
- the yield strength of steel changes with temperature according to the diagram illustrated in EN 1992-1-2 [7], Fig. 4.2a,

- the temperature of the reinforcement is assumed to be equal to the temperature of the concrete in the position of the cross-section, where the center of the rebar is located.

When using the 500°C isotherm method, firstly it is necessary to obtain the temperature distribution profile of the cross-section at required time step. That can be easily done by a thermal analysis of the cross-section using some of the existing programs, such as TempAnalysis [17]. An example of the temperature profile generated from TempAnalysis [17] for a reinforced concrete slab of height $h = 200$ mm, which is exposed to a nominal standard fire curve ISO 834 at time $t = 120$ min is shown in Figure 1.

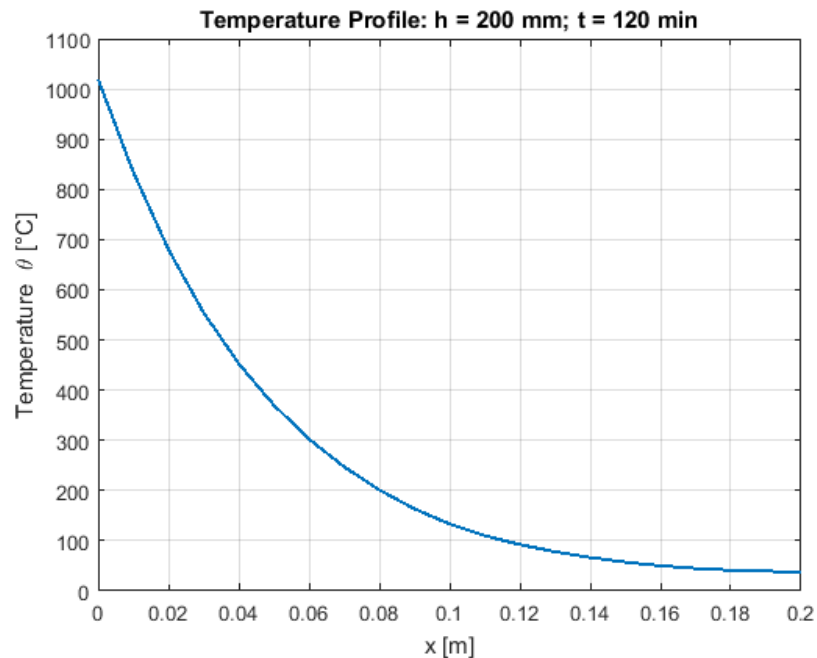


Figure 1 Temperature profile (generated from [17])

From the temperature profile, it is clear, that the temperature limit of 500°C is at the distance $a_{500} = 35$ mm from the surface. The new height of the cross-section is

$$h_{fi} = h - a_{500} = 200 - 35 = 165 \text{ mm.} \quad (3.1)$$

Let us assume that the slab is reinforced by steel bars, whose axial length from the lower surface is $a = 30$ mm. In that case, according to the temperature profile, the temperature of the reinforcement is $\theta = 550$ °C. The reduction coefficient of the characteristic yield strength $k_s(\theta)$ is obtained from EN 1992-1-2 [7], Fig. 4.2a which is shown in Figure 2.

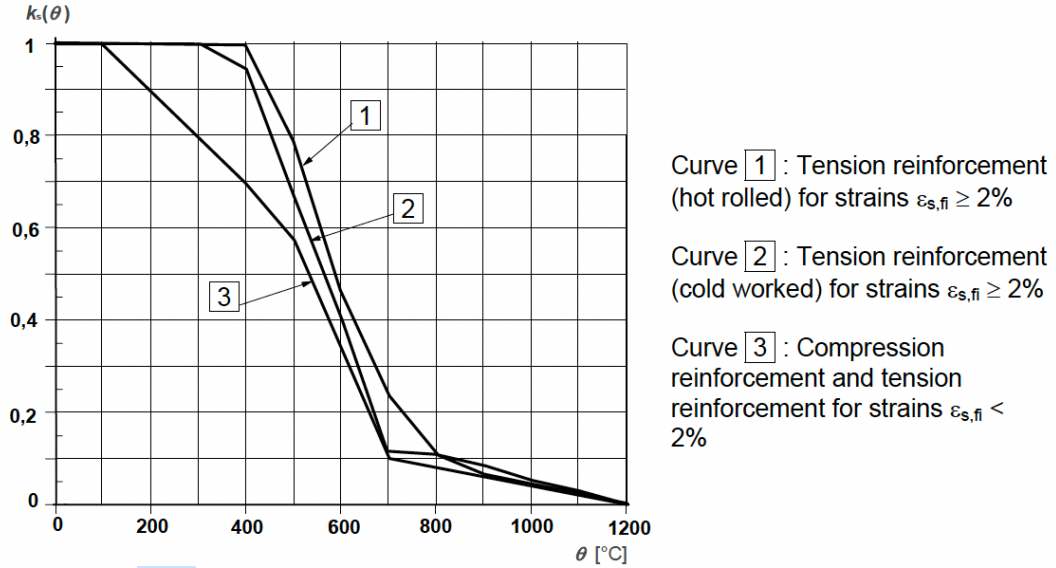


Figure 2 Coefficient $k_s(\theta)$ allowing for decrease of characteristic strength f_{yk} (taken from [7])

According to this diagram (curve number 1), the reduced yield strength of reinforcement is

$$f_{sy,\theta} = k_s(\theta) f_{yk} = 0.63 f_{yk} = 315 \text{ MPa}, \quad (3.2)$$

assuming that $f_{yk} = 500 \text{ MPa}$. This reduced yield strength is used in the relation for moment capacity calculation

$$M_{Rd,fi} = A_s f_{syd,\theta} z_{fi} = A_s \frac{f_{sy,\theta}}{\gamma_{S,fi}} z_{fi}, \quad (3.3)$$

where z_{fi} is the distance between internal forces after the cross-section dimension reduction and $\gamma_{S,fi}$ the coefficient of the reinforcement reliability during fire ($\gamma_{S,fi} = 1$).

Eventually, the moment capacity $M_{Rd,fi}$ is compared to the applied bending moment in a fire situation $M_{Ed,fi}$ to determine whether the load-bearing capacity of the element at a given time step is sufficient.

3.2.2 Zone method

This method is based on similar assumptions as the 500°C isotherm method, with some differences:

- structure is subjected to standard fire curve ISO 834 defined in EN 1991-1-2 [6],
- the cross-section dimensions are reduced with accordance to the so-called *mean reduction coefficient* $k_{c,m}$,
- the strength of concrete in the remaining part of the cross-section correspond to the reduced strength for temperature in the least heated part of the cross-section,
- the yield strength of steel changes with temperature according to the diagram illustrated in EN 1992-1-2 [7], Fig. 4.2a,
- the temperature of the reinforcement is assumed to be equal to the temperature of the concrete in the position of the cross-section, where the center of the rebar is located.

Firstly, the location of a point M in the cross-section is determined. The point is always located in the least heated part of the cross-section. If the element is exposed to fire from one side, the point M is located on the opposite surface, if the exposure is two-sided, the point M is in the center of the cross-section, as shown in Figure 3.

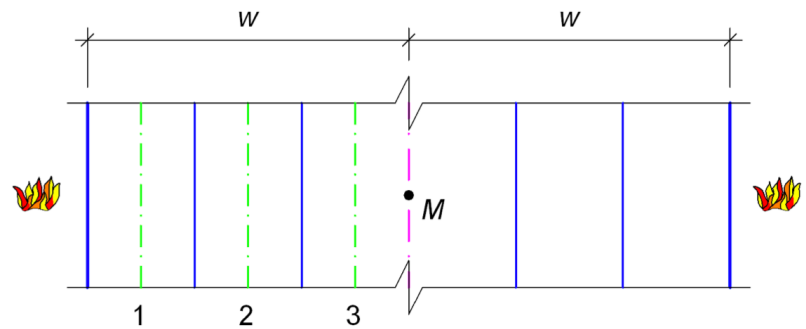


Figure 3 Cross-section division (taken from [8])

The characteristic thickness w is determined according to the location of the point M , as shown in Figure 3. This thickness is then divided into at least three zones of the same width. In the center of each zone the temperature of the concrete is found from the temperature profile of the cross-section.

For the center of each zone, the reduction coefficient of the characteristic concrete strength $k_{ci}(\theta)$ is obtained from EN 1992-1-2 [7], Fig. 4.1, which is shown in Figure 4.

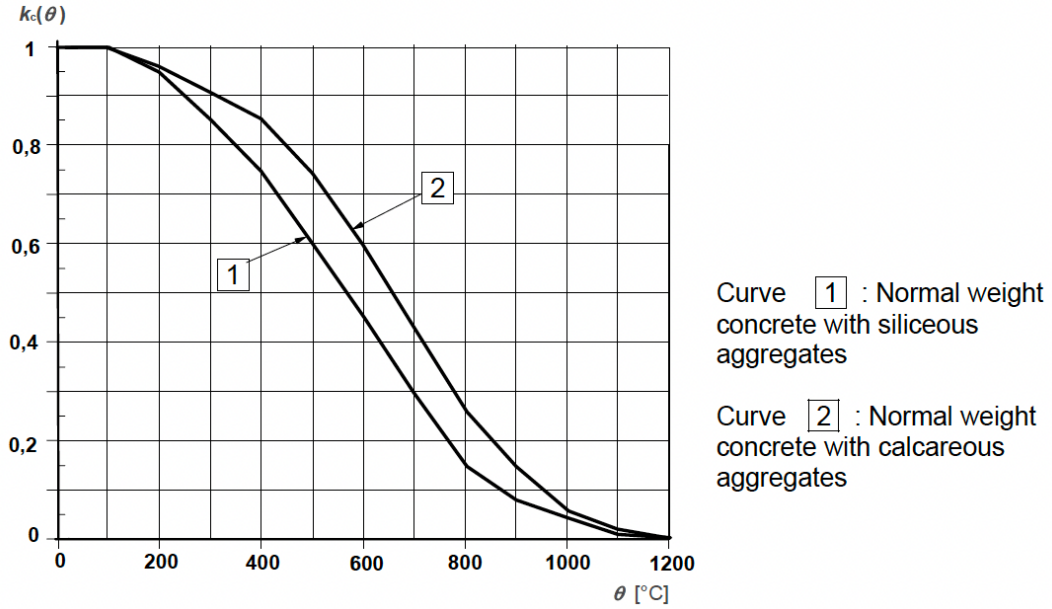


Figure 4 Coefficient $k_c(\theta)$ allowing for decrease of characteristic strength f_{ck} (taken from [7])

From $k_{ci}(\theta)$, the mean reduction coefficient $k_{c,m}$ can be obtained using the relation

$$k_{c,m} = \frac{1-0.2}{n} \sum_{i=1}^n k_{ci}(\theta), \quad (3.4)$$

where n stands for the number of zones.

The thickness of the eliminated layer of the cross-section a_z is determined from the equations

$$a_z = w \left(1 - \frac{k_{c,m}}{k_{c,\theta,M}} \right) \text{ and} \quad (3.5)$$

$$a_z = w \left(1 - \frac{k_{c,m}}{k_{c,\theta,M}} \right)^{1.3}, \quad (3.6)$$

where $k_{c,\theta,M}$ is a strength reduction coefficient of the point M . The equation used in each specific case depends on the type of the analyzed member (see [7]).

In cross-section of reduced dimensions, the concrete strength is reduced to correspond to the temperature at M , that is

$$f_{cd,fi} = k_{c,\theta,M} \frac{f_{ck}}{\gamma_{C,fi}}, \quad (3.7)$$

where $\gamma_{C,fi}$ is the coefficient of the concrete reliability during fire ($\gamma_{C,fi} = 1$).

3.2.3 Method for columns based on a curvature estimate

This method is usually used for analyzing columns whose behavior is influenced by the second order effects. It is only applicable for columns as part of solidified structures (EN 1992-1-2 [7]).

Similarly to the previous methods, firstly, it is necessary to obtain the temperature distribution profile of the cross-section at a required time step. For a constant axial force, the moment-curvature dependency is calculated with use of diagrams illustrated in EN 1992-1-2 [7] (step by step description provide chapters 6 and 7). For each curvature the equilibrium of internal and external forces is found. The moment of the internal forces around the center of the cross-section is the searched moment capacity $M_{Rd,fi}$. The difference between ultimate moment capacity $M_{Rd,fi}$ and nominal second order moment $M_{2,fi}$ is a first order moment capacity $M_{0Rd,fi}$ (as illustrated in Figure 5) which is then compared to the design first order bending moment for fire conditions $M_{0Ed,fi}$ (EN 1992-1-2 [7]).

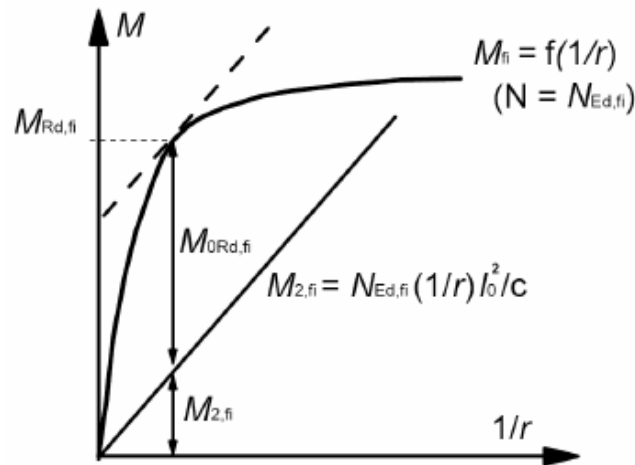


Figure 5 Determination of first order moment capacity $M_{0Rd,fi}$ (taken from [7])

4 Finite Element Method

4.1 Introduction to Finite Element Method

The Finite Element Method is one of the numerical methods for solving differential equations. Although originally developed for the purpose of mechanical analysis, it quickly expanded into other fields as well, and it now belongs to the most practiced methods in mechanics, thermodynamics, fluid dynamics or electromagnetism [4]. It can be traced back to the 1960s, when a textbook wearing the title *The Finite Element Method in Structural and Continuum Mechanics* was published. This was the very first textbook defining the basics of this method. A clear demonstration of the rapid evolution of FEM could be the fact that between the years 1971 and 2000 five editions of this textbook were published, with the last one exceeding the number of pages of the very first edition more than five times, despite significant reductions, according to [4].

Today the Finite Element Method stands and is accepted worldwide as a means of solving partial differential and integro-differential equations. Among its advantages counts its versatility in comparison with other methods, which qualifies FEM to solve various practical examples from many different fields and areas. Its finite number of elements means, that it is in general possible to obtain results quickly even in complex analyses with use of digital computational devices [4].

4.2 Principle of Finite Element Method

The basics of Finite Element Method lie in subdividing the system into individual elements. This is followed by the assembly and investigation of said system (see [4] and [5]).

Some systems can be accurately described with a model comprised of a finite number of correctly selected elements. These problems are called *discrete*. In other cases, the finite number of elements does not exist, and the system can be described only by mathematical fiction of an infinitesimal. These systems are called *continuous* [4].

We can also define a *standard discrete system*, which was developed over the years as a rather standard methodology for solving discrete problems. This methodology shows a certain pattern, which is applicable to discrete systems across different fields and areas [4].

This work focuses only on Finite Element Method in mechanics and thermodynamics.

In this chapter, the general concept of discrete systems is introduced through practical examples, which have been solved and coded in MATLAB [18] by the author of the thesis.

4.3 Finite Element Method in Thermal Analysis

Not only the force loads, but also the thermal loads have an impact on the mechanical response of a structure. With higher temperatures the material properties change, resulting in a greater vulnerability of the structure to the force loads. That is the reason for implementing thermal analysis into the complex mechanical analysis.

For this work a transient heat transfer is introduced. To explain the principle of FEM in thermal analysis, a simple illustrative example is presented.

Consider a ceiling composed of a reinforced concrete slab and a floor layer. All the material properties are known. Let the slab be subjected to heat flux, which is characterized as a time dependent function applied on the bottom surface.

The main aim of the analysis is to calculate temperature distribution along the cross-section at time $t = 30$ min.

The characteristic relation used for solving this problem can be written as

$$\mathbf{C}(\mathbf{x}^n) \frac{x^{n+1} - x^n}{\Delta t} + \mathbf{K}(\mathbf{x}^n) x^{n+1} + \mathbf{f} = 0, \quad (4.1)$$

where \mathbf{C} represents the heat capacity matrix and \mathbf{K} the thermal conductivity matrix, Δt is the specified time step, x^n and x^{n+1} stand for vectors of temperatures in each node at the actual and next time step. Finally, \mathbf{f} is the vector of heat flux which the structure is subjected to.

When analyzing the illustrative ceiling slab, a 500 mm long part of it served as a reference and representation of the behavior of the entire structure.

4.3.1 Mesh

As a first step it is necessary to generate mesh. The chosen fineness of the mesh is crucial since it has considerable impact on the obtained result. Too gross a mesh causes imprecise results, too fine a mesh results in greater computational costs [4].

When analyzing the illustrative example from the previous subchapter, for the purpose of this work the prevailing requirement was set to minimize the calculation time while the results remain intact. Therefore, for the analyzed characteristic part of the ceiling slab a mesh composed of 250 elements was generated as shown in Figure 6. To distinguish the different materials in the ceiling, the mesh is plotted in two colors. Yellow color stands for reinforced concrete (material A) and red color for the floor layer (material B).

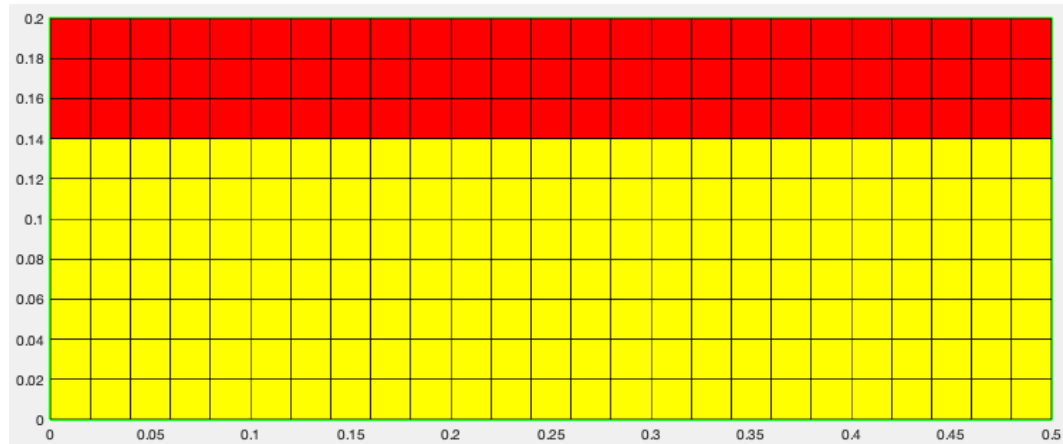


Figure 6 Mesh (created in [18])

4.3.2 Material parameters

After defining the geometry, it is necessary to assign to each layer its material characteristics. Specifically, the material parameters entering the calculation are density ρ , heat capacity c and conductivity λ .

Material parameters in the reference example are assigned as shown in Figure 7, where A stands for reinforced concrete and B for the floor layer.

```

7      % Material parameters
8 -    Dens_A = 2500; % [kg/(m3)] density
9 -    HCap_A = 1000; % [J/(kgK)] heat capacity
10 -   Cond_A = 1.5; % [W/(mK)] conductivity
11     %
12 -   Dens_B = 2000; % [kg/(m3)] density
13 -   HCap_B = 800; % [J/(kgK)] heat capacity
14 -   Cond_B = 1; % [W/(mK)] conductivity

```

Figure 7 Material parameters assigned to reinforced concrete (A) and floor layer (B)

4.3.3 Boundary conditions

The structure is subjected to a heat flux, which is for the purpose of this work defined as a time dependent function as shown in Figure 8.

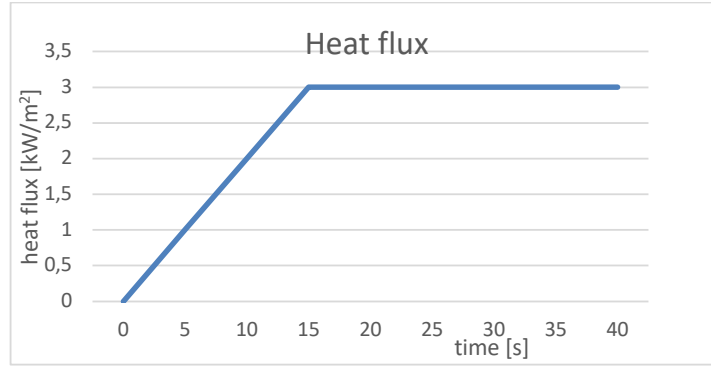


Figure 8 Function of the heat flux

The predefined heat flux is applied to selected nodes on the bottom surface of the structure.

4.3.4 Thermal analysis of the structure

The aim of this analysis is to calculate the temperature distribution at time $t = 30$ min using the relation (4.1).

Heat capacity matrix \mathbf{C} of an element takes the form of

$$\mathbf{C} = \frac{\rho c}{9} \begin{bmatrix} 4ab & 2ab & ab & 2ab \\ 2ab & 4ab & 2ab & ab \\ ab & 2ab & 4ab & 2ab \\ 2ab & ab & 2ab & 4ab \end{bmatrix}, \quad (4.2)$$

where a is calculated as a half of an element size in the direction of x axis, and b is calculated as a half of an element size in the direction of y axis.

Thermal conductivity matrix \mathbf{K} of an element takes the form of

$$\mathbf{K} = \lambda \begin{bmatrix} \frac{a}{3b} + \frac{b}{3a} & \frac{a}{6b} - \frac{b}{3a} & -\frac{a}{6b} - \frac{b}{6a} & -\frac{a}{3b} + \frac{b}{6a} \\ \frac{a}{6b} - \frac{b}{3a} & \frac{a}{3b} + \frac{b}{3a} & -\frac{a}{3b} + \frac{b}{6a} & \frac{a}{6b} - \frac{b}{6a} \\ -\frac{a}{6b} - \frac{b}{6a} & -\frac{a}{3b} + \frac{b}{6a} & \frac{a}{3b} + \frac{b}{3a} & \frac{a}{6b} - \frac{b}{3a} \\ -\frac{a}{3b} + \frac{b}{6a} & \frac{a}{6b} - \frac{b}{6a} & \frac{a}{6b} - \frac{b}{3a} & \frac{a}{3b} + \frac{b}{3a} \end{bmatrix}, \quad (4.3)$$

where a is calculated as a half of an element size in the direction of x axis, and b is calculated as a half of an element size in the direction of y axis.

The calculated temperature distribution along the cross-section at $t = 30$ min shows Figure 9.

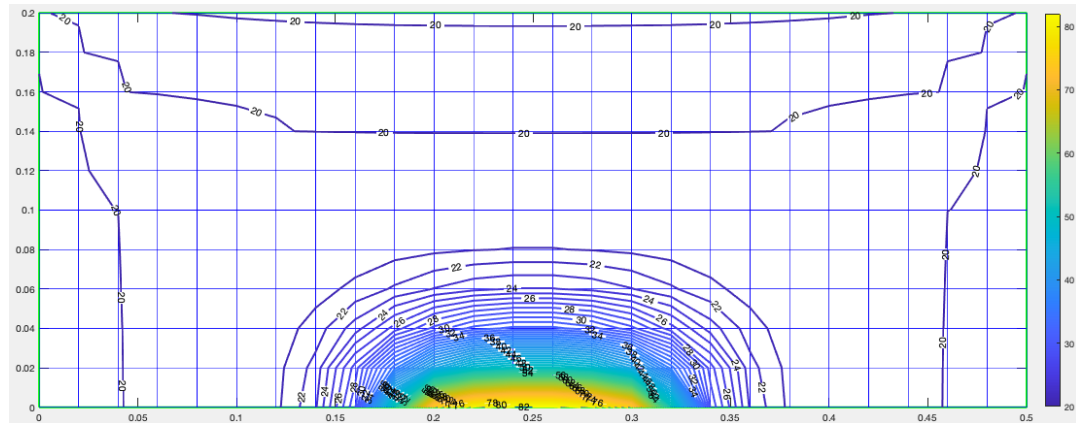


Figure 9 Temperature distribution in the cross-section at $t = 30$ min (created in [18])

The curves across the cross-section are so-called *isotherms*, which connect parts of the cross-section of the same temperatures.

4.3.5 Conclusion

This subchapter includes a calculation of the temperature distribution along the cross-section of a ceiling slab composed of a lower reinforced concrete slab and an upper floor layer subjected to a defined heat flux. A characteristic 500 mm long part of the structure was selected for the analysis. The example demonstrates the calculation of transient heat transfer.

From the graphic output it is evident that the temperatures in the cross-section of the slab are highest in the close vicinity of the applied heat flux, whereas further from the thermal load temperatures remain at the initial value of 20°C even after 30 minutes of exposure. Were the structure subjected to a heat flux of a higher value or for a longer amount of time, the temperatures would increase overall.

5 Mechanical Analysis

5.1 Structural Element

In this chapter, mechanical analysis of structures is introduced through several illustrative examples.

The first example is taken from [9]. Consider a two-dimensional structure as shown in Figure 10. For now, a linear elastic behavior is assumed, which is described as a linear relationship between the input (applied force, stress) and the output (displacement, strain) [10]. The cross-sectional area and Young's modulus of the material are both known. Let the truss be subjected to a force F of a given value. The joints are pinned, so that moments cannot be transmitted within the bars.

As was explained in chapter 4.2, the system is firstly subdivided into individual elements. In this case the subdivision is very simple. The structure comprises of two bars, thus two elements. There are nodes on either end of each element.

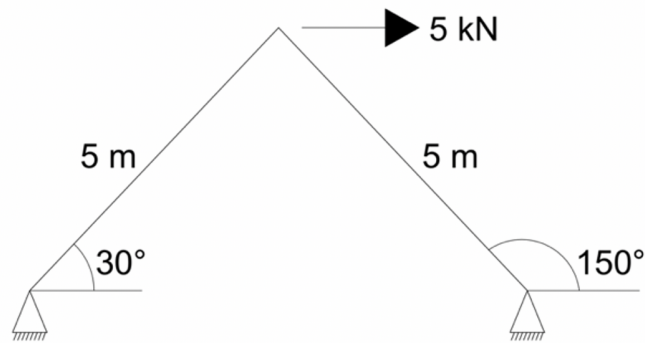


Figure 10 Truss structure subjected to mechanical loading

Firstly, to investigate the structure, it is necessary to assign numbers to all the elements and nodes. The order in which the numbers are assigned does not matter. For example, in this case the numbers were assigned as shown in Figure 11.

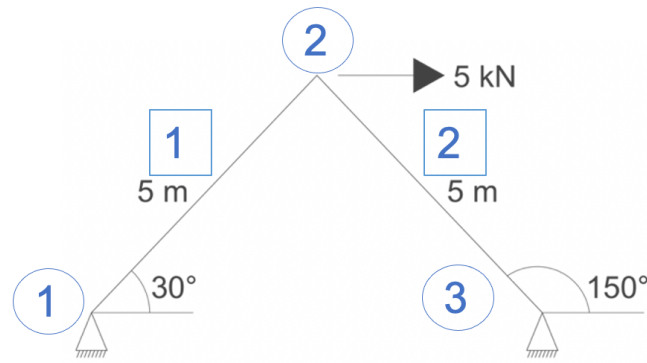


Figure 11 Numbers assigned to elements and nodes

Assuming linear elastic behavior of the element, the system of equations describing the relationship always takes form of

$$\mathbf{K} \mathbf{u} = \mathbf{f}, \quad (5.1)$$

where \mathbf{K} stands for the *element stiffness matrix*, \mathbf{f} represents the vector of nodal external forces and \mathbf{u} the vector of corresponding nodal displacements of the element. The size of the element stiffness matrix depends on the number of degrees of freedom of the element. As in the two-dimensional problem, each node is defined by two degrees of freedom and the element is interconnected with two nodes, the element stiffness matrix is of the size 4×4 . Let C be the cosine of the angle between the element and the x axis and S the sine of the same angle, then

$$\mathbf{K}^e = \frac{EA}{L} \begin{bmatrix} C^2 & CS & -C^2 & -CS \\ CS & S^2 & -CS & -S^2 \\ -C^2 & -CS & C^2 & CS \\ -CS & -S^2 & CS & S^2 \end{bmatrix}, \quad (5.2)$$

where E is the Young's modulus of material, A is the cross-sectional area and L the length of the element.

5.1.1 Assembly and analysis of the structure

In the next step the structure is assembled and analyzed. To obtain the solution, we must satisfy the following conditions:

- 1) displacement compatibility and
- 2) equilibrium.

According to [4], any system of nodal displacements \mathbf{u} listed for the whole structure in which all the elements participate automatically satisfies the condition of displacement compatibility. Since the conditions of equilibrium within an element have been already

satisfied, it is only necessary to establish equilibrium conditions at the nodes of the structure.

Considering the structure as shown in Figure 10, the corresponding vector of nodal displacement is

$$\mathbf{u} = \begin{Bmatrix} u_{x1} \\ u_{y1} \\ u_{x2} \\ u_{y2} \\ u_{x3} \\ u_{y3} \end{Bmatrix}, \quad (5.3)$$

and the corresponding vector of external nodal forces is

$$\mathbf{f} = \begin{Bmatrix} f_{x1} \\ f_{y1} \\ f_{x2} \\ f_{y2} \\ f_{x3} \\ f_{y3} \end{Bmatrix}, \quad (5.4)$$

where $f_{x2} = 5$ kN.

The assembly process is the fundamental feature of all finite element calculations. It is crucial to assemble the stiffness matrix of the whole structure. This matrix is called the *global stiffness matrix* [4].

The global stiffness matrix of the reference structure is of the size 6×6 (three nodes, each two degrees of freedom) and takes form of

$$\mathbf{K} = \begin{bmatrix} K_{11}^1 & K_{12}^1 & K_{13}^1 & K_{14}^1 & 0 & 0 \\ K_{21}^1 & K_{22}^1 & K_{23}^1 & K_{24}^1 & 0 & 0 \\ K_{31}^1 & K_{32}^1 & K_{33}^1 + K_{11}^2 & K_{34}^1 + K_{12}^2 & K_{13}^2 & K_{14}^2 \\ K_{41}^1 & K_{42}^1 & K_{43}^1 + K_{21}^2 & K_{44}^1 + K_{22}^2 & K_{23}^2 & K_{24}^2 \\ 0 & 0 & K_{31}^2 & K_{32}^2 & K_{33}^2 & K_{34}^2 \\ 0 & 0 & K_{41}^2 & K_{42}^2 & K_{43}^2 & K_{44}^2 \end{bmatrix} \quad (5.5)$$

5.1.2 Boundary conditions

In some cases, a certain displacement is described. For that we use the term *constraint condition*. The simplest constraint condition is the so-called *single-freedom constraint*. Through the single-freedom constraint we impose a prescribed value for one nodal displacement component. The term *homogeneous condition* is used when the equation prescribing the displacement equals zero. For instance

$$u_{x1} = 0. \quad (5.6)$$

The term *non-homogeneous condition* is used when the equation prescribing the displacement is not equal to zero. For example

$$u_{x1} = 4, u_{y1} = 0.7. \quad (5.7)$$

The usual solution for a single-freedom constraint is deleting the appropriate row and column corresponding to the restricted displacement in the stiffness matrix and the vectors \mathbf{u} and \mathbf{f} and thus reducing the system of equations.

More complex constraint condition is the so-called *multi-freedom constraint*. The multi-freedom constraint is a functional equation, which connects two or more displacement components. For instance

$$u_{x1} + u_{x3} = 0, u_{y2} + u_{x4} = 5.2 \quad (5.8)$$

are multi-freedom constraints, first one is homogeneous while the second one non-homogeneous.

There are multiple ways of treating the multi-freedom constraints. For the purpose of this work the *Lagrange Multiplier Adjunction* is described.

Lagrange Multiplier Adjunction belongs to the methods for imposing single-freedom and multi-freedom constraints. In principle, for each constraint an additional variable or a set of variables is appended to the stiffness equations. Said variables represent constraint forces, which, if applied to the unconstrained system, would enforce the constraints. The Lagrange multiplier λ is appended to the vector of original unknowns. The set of equation with adjoined unknowns is called the *multiplier-augmented system*. The process of appending λ to the vector of unknowns is called *adjunction*. Through solving the system, the solution for the degrees of freedom is obtained and the constraint forces are characterized through λ .

The boundary conditions in the illustrative example from Figure 10 resulting from the supporting conditions prescribe following constraint:

$$u_{x1} = u_{y1} = u_{x3} = u_{y3} = 0. \quad (5.9)$$

Thus, the only unknown displacements are u_{x2} and u_{y2} . After inserting the boundary conditions to the equations, the structure can be solved for these unknown displacements.

5.1.3 Conclusion

In this subchapter the deformation of a basic two-dimensional truss structure with assumption of a linear elastic behavior was calculated. A linear behavior means that the relationship between the input such as applied forces and stress, and the output such as displacements and strain is linear. The procedure applied to obtain

the unknown variables (nodal displacements) is called *the direct stiffness method* and it is a typical method used for analysis of structures with linear elastic behavior.

5.2 Nonlinear mechanical analysis

Nonlinear systems are defined with a nonlinear relationship between the input and the output [10]. Generally, there are four types of nonlinearities defined in structural mechanics according to [10]:

Geometric nonlinearity is a nonlinearity among displacement, rotation, and strain. It usually occurs together with large deformation.

Material nonlinearity means that the relationship between stress and strain is nonlinear. This relationship usually takes a graphic form of a stress-strain diagram. Material nonlinearity is typical for many materials including concrete and steel.

Kinematic nonlinearity occurs when the displacement boundary conditions depend on deformation of the structure.

Force nonlinearity represents the case when the applied forces depend on deformation.

To explain the nonlinear analysis, consider a one-dimensional example as shown in the Figure 12. This example is taken from [10].

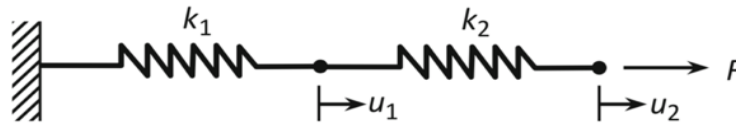


Figure 12 Serially connected nonlinear springs (taken from [10])

In this example, two serially connected nonlinear spring elements are pulled by an applied force $F = 100$ N. The variables are the elongations of springs u_1 and u_2 . Assume that the stiffness of both springs depends on the elongation such that $k_1 = 50 + 500 u$ and $k_2 = 100 + 200 u$ (N/m).

The elongation is solved using the same relation as in the linear analysis, which takes the form of

$$\mathbf{K} \mathbf{u} = \mathbf{f}, \quad (5.10)$$

where the element stiffness matrix is

$$\mathbf{K}^e = \begin{bmatrix} k & -k \\ -k & k \end{bmatrix}. \quad (5.11)$$

While the elongation of spring 1 is u_1 , the elongation of spring 2 is $u_2 - u_1$.

5.2.1 Assembly

Considering the structure as shown in Figure 12, the corresponding vector of nodal displacement is

$$\mathbf{u} = \begin{Bmatrix} u_0 \\ u_1 \\ u_2 \end{Bmatrix}, \quad (5.12)$$

and the corresponding vector of external nodal forces is

$$\mathbf{f} = \begin{Bmatrix} f_0 \\ f_1 \\ f_2 \end{Bmatrix}, \quad (5.13)$$

where $f_2 = 100$ N.

The global stiffness matrix of the reference structure is of the size 3×3 (three nodes, each one degree of freedom) and is in the form

$$\mathbf{K} = \begin{bmatrix} k_1 & -k_1 & 0 \\ -k_1 & k_1 + k_2 & -k_2 \\ 0 & -k_2 & k_2 \end{bmatrix}. \quad (5.14)$$

5.2.2 Boundary conditions

Since spring 1 is fixed, the boundary conditions in the illustrative example from Figure 12 resulting from the supporting conditions prescribe following constraint:

$$u_0 = 0. \quad (5.15)$$

It is a single-freedom constraint which is, in this example, treated by deleting the appropriate row and column corresponding to the restricted displacement in the stiffness matrix and both vectors and thus reducing the set of equations.

By multiplying the stiffness matrix and the vector of unknown displacements, the following set of equations is obtained:

$$\begin{aligned} 300u_1^2 + 400u_1u_2 - 200u_2^2 + 150u_1 - 100u_2 &= 0 \\ 200u_1^2 - 400u_1u_2 + 200u_2^2 - 100u_1 + 100u_2 &= 100. \end{aligned} \quad (5.16)$$

5.2.3 Analysis of a nonlinear structure

To find roots of nonlinear equations, one of the procedures for solving a system of nonlinear equations must be implemented. One of the most popular methods in the numerical analysis is *Newton* or *Newton-Raphson method*, which is also used for solving the reference example from Figure 12.

Newton method is a numerical method based on the principle of iterations. Its fundament is an assumption of an initial estimate \mathbf{u}^0 of the variables. Consequently, the nonlinear equations are locally approximated by linear ones to find the increment $\Delta\mathbf{u}$ to the initial estimate. The new estimate $\mathbf{u}^0 + \Delta\mathbf{u}$ is closer to satisfying the nonlinear equation. Through repeating this process, the estimate converges to the accurate solution until the required tolerance is satisfied [10].

First step when using Newton method is setting the required tolerance of the solution and the value of the initial estimate. Then the so-called residual R is calculated using the relation

$$\mathbf{R} = \mathbf{f} - \mathbf{P}(\mathbf{u}), \quad (5.17)$$

where $\mathbf{P}(\mathbf{u})$ is an internal force vector which depends on the elongation \mathbf{u} .

Afterwards the matrix \mathbf{K}_T , which is called Jacobian matrix, is calculated as

$$\mathbf{K}_T(\mathbf{u}) = (\partial\mathbf{P}/\partial\mathbf{u}). \quad (5.18)$$

By solving the equation

$$\mathbf{K}_T\Delta\mathbf{u} = \mathbf{f} - \mathbf{P}(\mathbf{u}), \quad (5.19)$$

the increment $\Delta\mathbf{u}$ is calculated which updates the solution by

$$\mathbf{u} = \mathbf{u} + \Delta\mathbf{u}. \quad (5.20)$$

If the new \mathbf{u} meets the solution with required tolerance, the calculation is finished and the \mathbf{u} from the last iteration is considered as the final solution [10].

Newton Raphson method is usually implemented with use of computational devices. The method is computationally quite demanding especially since the two most complex operations, forming the Jacobian matrix, and solving the matrix equation are repeated at every iteration. To decrease the complexity and shorten the calculation time when using computational devices, the modified Newton method was introduced [10].

While the regular Newton method requires the Jacobian matrix to be formed at each iteration, the modified Newton method builds the Jacobian matrix only once at the beginning and then uses the initial matrix repeatedly in each iteration [10].

Using the initial matrix repeatedly through the process causes greater number of iterations required for solving the equations. However, the absence of building the Jacobian matrix in every iteration shortens the required time for each iteration and overall reduces the computational cost of the process [10].

The reference example is solved using both Newton and modified Newton method to compare the results.

The initial estimate was in both cases set to

$$\mathbf{u}_0 = \begin{Bmatrix} u_1 \\ u_2 \end{Bmatrix} = \begin{Bmatrix} 0.1 \\ 0.5 \end{Bmatrix} \text{ m.} \quad (5.21)$$

Figure 13 shows the unknown displacements obtained by implementing the Newton method. The final displacements u_1 and u_2 were reached with the required tolerance after five iterations.

iteration	u1	u2
1	0.10000	0.50000
2	0.70000	1.20769
3	0.46000	0.96004
4	0.40353	0.90353
5	0.40001	0.90001
6	0.40000	0.90000>>

Figure 13 Results obtained using Newton method

Figure 14 shows the unknown displacements obtained by implementing the modified Newton method. The final displacements u_1 and u_2 were reached with the required tolerance after ten iterations.

iteration	u1	u2
1	0.10000	0.50000
2	0.35714	0.88442
3	0.40962	0.89903
4	0.39712	0.90087
5	0.40081	0.89943
6	0.39977	0.90027
7	0.40007	0.89988
8	0.39998	0.90005
9	0.40001	0.89998
10	0.40000	0.90001
11	0.40000	0.90000>>

Figure 14 Results obtained using modified Newton method

For illustration, Figure 15 shows the official results of this example as presented in [10].

Iteration	u_1	u_2	conv	c
0	0.0000	0.0000	9.999E-01	-
1	2.0000	3.0000	3.280E+02	-
2	1.0244	1.6244	1.981E+01	0.164
3	0.5814	1.0873	9.282E-01	0.357
4	0.4261	0.9261	1.455E-02	0.744
5	0.4007	0.9007	1.033E-05	1.048
6	0.4000	0.9000	6.462E-12	1.109

Figure 15 Official results (taken from [10])

Even though the initial estimate is in our case different from the one presented in [10], it is clear that the algorithm came to the same values of unknown displacements, which proves that the algorithm calculates with sufficient accuracy.

5.2.4 Conclusion

In this subchapter, the deformation of two serially connected nonlinear spring elements was calculated. To compare different solving methods, the unknown displacements were obtained using both regular and modified Newton-Raphson method.

Whilst defining the same input, initial estimate of variables and required tolerance in both methods, a difference between the number of iterations required to obtain the solution was detected. The final solution was obtained in five iterations using the regular Newton method, whereas ten iterations were required to get the solution using the modified Newton method. No difference in computational time was detected, which is due to simplicity of the reference example. It is presumed, that the difference would grow with the complexity of analyzed structure in favor to modified Newton method.

5.3 Direct Stiffness Method in truss mechanical analysis

This subchapter deals with a mechanical analysis of several truss structures exposed to mechanical and thermal loadings. The procedure implemented for all the following examples is the so-called *direct stiffness method* (see [5]) and it will be closely described later in this chapter. The following examples are based on the following assumptions:

- linear material properties of both concrete and steel,
- material properties do not change with increasing temperatures.

The first example which is presented here is taken from [11]. Consider a truss structure comprised of 5 bars, as shown in Figure 16. The cross-sectional area and Young's modulus of the material are both known.

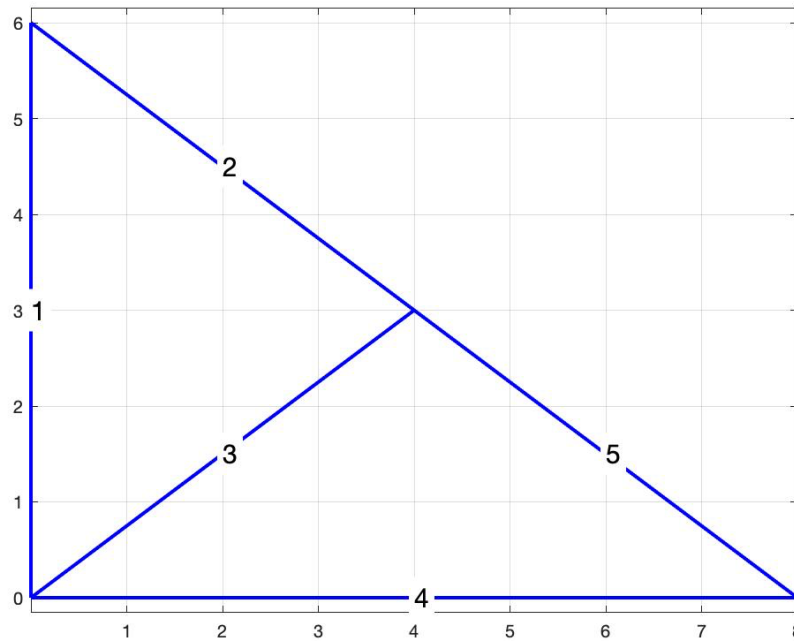


Figure 16 Truss structure (created in [18])

5.3.1 Mechanical analysis – prescribed force

The direct stiffness method is best described through an example taken from [11]. For all the following examples assume $EA = 1 \text{ N}$.

Let us assume that the structure is subjected to a force $F = 1 \text{ N}$ in node number 4 according to Figure 17.

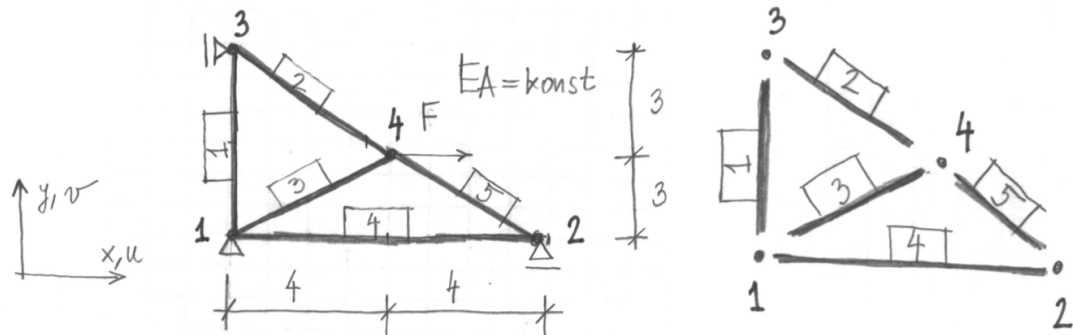


Figure 17 Element numbers and force in node 4 (taken from [11])

Firstly, it is necessary to assign the so-called *code numbers* to the global nodal displacements. All the unknown displacements are given numbers starting from 1. Where the boundary conditions prescribe a displacement as zero, the code number for this displacement is a zero as well, as shown in Figure 18.

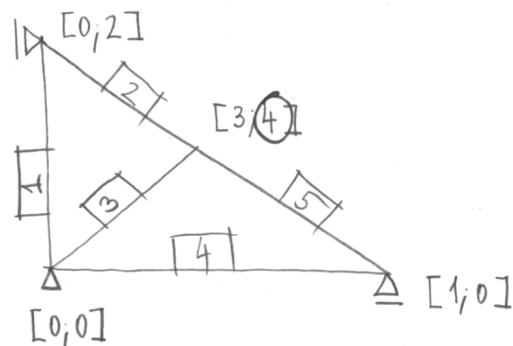


Figure 18 Code numbers (taken from [11])

The corresponding vector of unknown nodal displacements is

$$\mathbf{u} = \begin{Bmatrix} u_{x1} \\ u_{y2} \\ u_{x3} \\ u_{y4} \end{Bmatrix}, \quad (5.22)$$

and the corresponding vector of external nodal forces is

$$\mathbf{f} = \begin{Bmatrix} 0 \\ 0 \\ 1 \\ 0 \end{Bmatrix}. \quad (5.23)$$

The global stiffness matrix of the size of 4×4 is assembled and it looks as following:

$$\mathbf{K} = \begin{bmatrix} 0.253 & 0 & -0.128 & 0.096 \\ 0 & 0.239 & 0.096 & -0.072 \\ -0.128 & 0.096 & 0.384 & -0.096 \\ 0.096 & -0.072 & -0.096 & 0.216 \end{bmatrix} \text{ N/m}. \quad (5.24)$$

After applying the solving formula which takes the form of

$$\mathbf{u} = \mathbf{K} \backslash \mathbf{f}, \quad (5.25)$$

where \backslash is a *backslash operator* used in MATLAB [18] for solving systems of linear equations, we get following nodal displacements:

$$\mathbf{u} = \begin{Bmatrix} 1.657 \\ -1.318 \\ 3.591 \\ 0.420 \end{Bmatrix} \text{ m}. \quad (5.26)$$

5.3.2 Mechanical analysis – prescribed force, reactions

To obtain reactions in the supports, a different approach is needed.

Let us assume the same structure subjected to a force $F = 1$ N. This time, the code numbers given to each displacement differ. Lower numbers are used to indicate unconstrained degrees of freedom. Firstly, let us assign a number to each unknown displacement, starting from number 1. After assigning every unknown displacement with a code number, we proceed to give code numbers to the known displacements, resulting in them being assigned the largest numbers. Compared to the previous example, where known displacements are assigned with a zero, this way the known displacements are not eliminated from the stiffness matrix. Instead, the vectors and matrix are divided into known and unknown parts.

The code numbers are assigned as shows Figure 19.

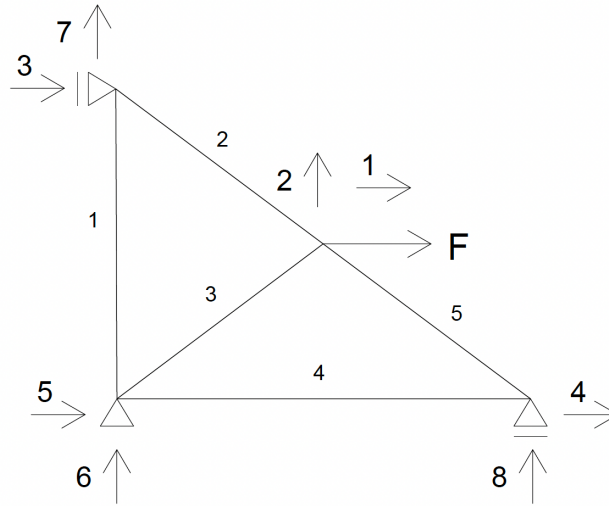


Figure 19 Example with prescribed force

The corresponding vector of both unknown and known nodal displacements is

$$\mathbf{d} = \begin{Bmatrix} u_{x1} \\ u_{y2} \\ u_{y3} \\ u_{x4} \\ k_{x5} \\ k_{y6} \\ k_{x7} \\ k_{y8} \end{Bmatrix}, \quad (5.27)$$

where u stands for unknown and k for known displacements, and the corresponding vector of nodal forces and reactions is

$$\mathbf{f} = \begin{Bmatrix} 1 \\ 0 \\ 0 \\ 0 \\ r_{x5} \\ r_{y6} \\ r_{x7} \\ r_{y8} \end{Bmatrix} \text{ N}, \quad (5.28)$$

where r stands for reactions and numbers 1 and 0 for external forces in the nodes.

The global stiffness matrix of the size of 8×8 is assembled and it looks as following:

$$\mathbf{K} = \begin{bmatrix} 0.384 & -0.096 & 0.096 & -0.128 & -0.128 & -0.096 & -0.128 & 0.096 \\ -0.096 & 0.216 & -0.072 & 0.096 & -0.096 & -0.072 & 0.096 & -0.072 \\ 0.096 & -0.072 & 0.239 & 0 & 0 & -0.167 & -0.096 & 0 \\ -0.128 & 0.096 & 0 & 0.253 & -0.125 & 0 & 0 & -0.096 \\ -0.128 & -0.096 & 0 & -0.125 & 0.253 & 0.096 & 0 & 0 \\ -0.096 & -0.072 & -0.167 & 0 & 0.096 & 0.239 & 0 & 0 \\ -0.128 & 0.096 & -0.096 & 0 & 0 & 0 & 0.128 & 0 \\ 0.096 & -0.072 & 0 & -0.096 & 0 & 0 & 0 & 0.072 \end{bmatrix} \text{ N/m.} \quad (5.29)$$

To calculate the displacements and obtain the reactions in the supports, it is necessary to split both vectors as implied in the known and unknown parts. That means the vector \mathbf{d} is split to unknown and known displacements \mathbf{u} and \mathbf{k} , the vector \mathbf{f} to known external forces \mathbf{F} and unknown reactions in supports \mathbf{R} . The stiffness matrix \mathbf{K} needs to be split in four parts to correspond with the vectors. In the reference example, in each vector, there are four known and four unknown values, so the matrix is split into four parts, each of the size 4×4 , which is illustrated in Figure 20.



Figure 20 Split of stiffness matrix

Firstly, the unknown displacements $u_{x1}, u_{y2}, u_{y3}, u_{x4}$ are calculated with use of

$$\mathbf{K}_{11} \mathbf{u} + \mathbf{K}_{12} \mathbf{k} = \mathbf{F}, \quad (5.30)$$

from which \mathbf{u} is formularized as

$$\mathbf{u} = \mathbf{K}_{11}(\mathbf{F} - \mathbf{K}_{12} \mathbf{k}). \quad (5.31)$$

After solving the unknown displacements as vector \mathbf{u}

$$\mathbf{u} = \begin{Bmatrix} 3.591 \\ 0.420 \\ -1.318 \\ 1.657 \\ 0 \\ 0 \\ 0 \\ 0 \end{Bmatrix} \text{ m,} \quad (5.32)$$

it is possible to calculate the reactions in the supports using the equation

$$\mathbf{R} = \mathbf{K}_{21} \mathbf{u} + \mathbf{K}_{22} \mathbf{k}. \quad (5.33)$$

After solving these equations, vector f is obtained with following values:

$$f = \begin{Bmatrix} 1 \\ 0 \\ 0 \\ 0 \\ r_{x5} \\ r_{y6} \\ r_{x7} \\ r_{y8} \end{Bmatrix} = \begin{Bmatrix} 1 \\ 0 \\ 0 \\ 0 \\ -0.707 \\ -0.155 \\ -0.293 \\ 0.155 \end{Bmatrix} \text{ N.} \quad (5.34)$$

5.3.3 Mechanical analysis – prescribed displacement, reactions

The approach described in the previous subchapter can be used in examples with prescribed displacements as well.

Assume the structure from previous chapters. Instead of an external force, this structure is subjected to a prescribed displacement as shown in Figure 21.

Let us assign code numbers 1–3 to unknown displacements and code numbers 4–8 to known displacements.

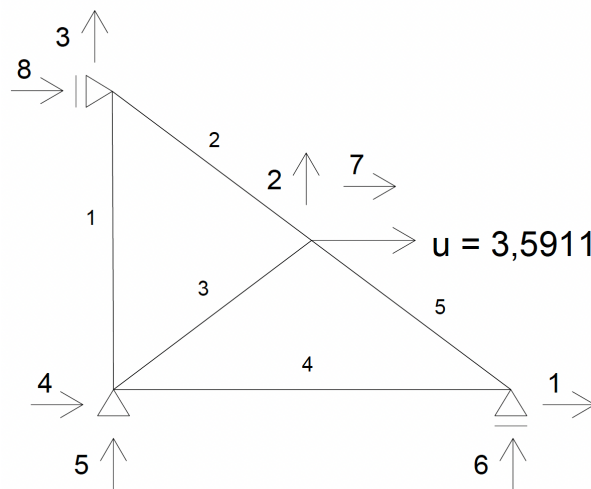


Figure 21 Example with prescribed displacement

The corresponding vector of both unknown and known nodal displacements is

$$d = \begin{Bmatrix} u_{x1} \\ u_{y2} \\ u_{y3} \\ k_{x4} \\ k_{y5} \\ k_{y6} \\ k_{x7} \\ k_{x8} \end{Bmatrix}, \quad (5.35)$$

and the corresponding vector of nodal forces and reactions is

$$\mathbf{f} = \begin{Bmatrix} 0 \\ 0 \\ 0 \\ r_{x4} \\ r_{y5} \\ r_{y6} \\ r_{x7} \\ r_{x8} \end{Bmatrix}. \quad (5.36)$$

The global stiffness matrix of the size of 8×8 is assembled and it looks as following:

$$\mathbf{K} = \begin{bmatrix} 0.253 & 0.096 & 0 & -0.125 & 0 & -0.096 & -0.128 & 0 \\ 0.096 & 0.216 & -0.072 & -0.096 & -0.072 & -0.072 & -0.096 & 0.096 \\ 0 & -0.072 & 0.239 & 0 & -0.167 & 0 & 0.096 & -0.096 \\ -0.125 & -0.096 & 0 & 0.253 & 0.096 & 0 & -0.128 & 0 \\ 0 & -0.072 & -0.167 & 0.96 & 0.239 & 0 & -0.096 & 0 \\ -0.096 & -0.072 & 0 & 0 & 0 & 0.072 & 0.096 & 0 \\ -0.128 & -0.096 & 0.096 & -0.128 & -0.096 & 0.096 & 0.384 & -0.128 \\ 0 & 0.096 & -0.096 & 0 & 0 & 0 & -0.128 & 0.128 \end{bmatrix} \text{ N/m.} \quad (5.37)$$

The vectors, as well as the stiffness matrix are split in the same way as described in the previous example.

After solving $\mathbf{u} = \mathbf{K}_{11}(\mathbf{F} - \mathbf{K}_{12} \mathbf{k})$ and $\mathbf{R} = \mathbf{K}_{21} \mathbf{u} + \mathbf{K}_{22} \mathbf{k}$, we obtain vector of displacements and vector of nodal forces and reactions as following:

$$\mathbf{u} = \begin{Bmatrix} 1.657 \\ 0.420 \\ -1.318 \\ 0 \\ 0 \\ 0 \\ 3.591 \\ 0 \end{Bmatrix} \text{ m, } \mathbf{f} = \begin{Bmatrix} 0 \\ 0 \\ 0 \\ -0.707 \\ -0.155 \\ 0.155 \\ 1 \\ -0.293 \end{Bmatrix} \text{ N.} \quad (5.38)$$

5.3.4 Mechanical analysis – prescribed force and thermal loading

Let us assume that the structure from the previous subchapters is subjected to a force $F = 1 \text{ N}$ in node number 3, and that all the bars are heated by 500°C , as shown in Figure 22.

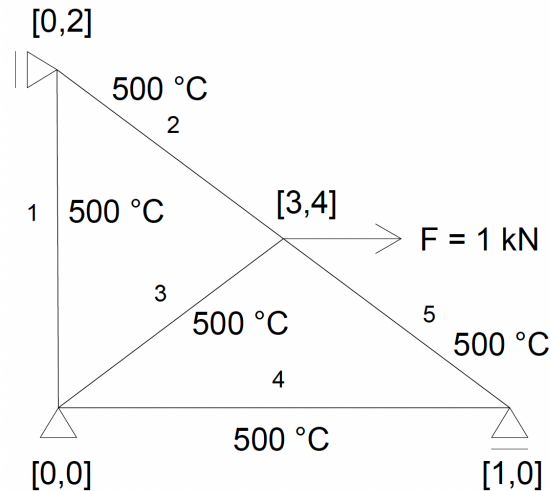


Figure 22 Example with prescribed force and thermal loading

The unknown displacements are solved with the use of relation

$$\mathbf{K} \mathbf{u} = \mathbf{f} - \mathbf{f}_t \quad (5.39)$$

where \mathbf{f}_t is a vector of forces in the nodes caused by the heat loading.

The corresponding vector of unknown nodal displacements is the same as (5.22), the corresponding vector of external nodal forces is the same as (5.23) and the global stiffness matrix of the size of 4×4 is assembled as (5.24).

The vector of forces caused by the heat is calculated for each element as

$$\mathbf{f}^e = E A \alpha L dT \begin{bmatrix} C & S \\ -C & -S \end{bmatrix} \quad (5.40)$$

where α is the **temperature coefficient**, L is the length of the element, dT the **temperature difference** in $^\circ\text{C}$ and C and S the cosine and sine of the angle between the element and the x axis.

From these element vectors \mathbf{f}^e the global vector of heat forces in the nodes can be assembled as

$$\mathbf{f}_t = \begin{Bmatrix} -0.072 \\ -0.54 \\ -0.024 \\ -0.018 \end{Bmatrix} \text{ N.} \quad (5.41)$$

Now it is possible to solve the equation (5.39), from which \mathbf{u} is formularized as

$$\mathbf{u} = \mathbf{K}(\mathbf{f} - \mathbf{f}_t). \quad (5.42)$$

The obtained vector of nodal displacements is

$$\mathbf{u} = \begin{Bmatrix} 1.991 \\ -1.130 \\ 3.733 \\ 0.481 \end{Bmatrix} \text{ m.} \quad (5.43)$$

5.3.5 Axial forces and deformation – force loading

From the displacements it is possible to calculate deformation of unconstrained elements, i.e. those with no restrictions preventing them from elongation, using the relation

$$\varepsilon = \frac{\Delta L}{L} = \frac{u_1 - u_2}{L}, \quad (5.44)$$

where ΔL is the elongation of the element and u_1, u_2 are local displacements of the element calculated from the global displacements as

$$\begin{Bmatrix} u_1 \\ u_2 \end{Bmatrix} = \begin{bmatrix} C & 0 \\ S & 0 \\ 0 & C \\ 0 & S \end{bmatrix} \setminus \begin{Bmatrix} u_{x1} \\ u_{y1} \\ u_{x2} \\ u_{y2} \end{Bmatrix}. \quad (5.45)$$

However, if the element is prevented from expansion, stress and internal forces develop in the element. This stress can be calculated using the equation

$$\sigma = E \varepsilon = E \frac{\Delta L}{L}. \quad (5.46)$$

By multiplying stress by the cross-sectional area, the axial force in the element is obtained:

$$N = \sigma A = E \varepsilon A = E \frac{\Delta L}{L} A. \quad (5.47)$$

If the stress value is positive, the element is in tension, otherwise it is in compression.

This is demonstrated using the example from previous subchapters. The truss is subjected to a force $F = 1 \text{ N}$.

After obtaining the vector of nodal displacements

$$\mathbf{u} = \begin{Bmatrix} 3.591 \\ 0.420 \\ -1.318 \\ 1.657 \\ 0 \\ 0 \\ 0 \\ 0 \end{Bmatrix} \text{ m}, \quad (5.48)$$

the axial force in each element can be obtained. Firstly, it is necessary to calculate the nodal displacements in local coordinate system. For example, for element (1) it is calculated as

$$\begin{Bmatrix} u_1 \\ u_2 \end{Bmatrix} = \begin{bmatrix} C & 0 \\ S & 0 \\ 0 & C \\ 0 & S \end{bmatrix} \begin{Bmatrix} u_{x5} \\ u_{y6} \\ u_{x7} \\ u_{y3} \end{Bmatrix} = \begin{bmatrix} C & 0 \\ S & 0 \\ 0 & C \\ 0 & S \end{bmatrix} \begin{Bmatrix} 0 \\ 0 \\ 0 \\ -1.318 \end{Bmatrix} = \begin{Bmatrix} 0 \\ -1.318 \end{Bmatrix} \text{ m}. \quad (5.49)$$

The axial force is then calculated from the equation (5.47) as

$$N = \sigma A = E \varepsilon A = E \frac{\Delta L}{L} A = 1 \frac{-1.3177-0}{6} = 0.2196 \text{ N}. \quad (5.50)$$

The axial forces in the rest of the elements are calculated identically.

5.3.6 Axial forces and deformation – force and thermal loading

With increasing temperature in the element, the element expands. If the element is mechanically prevented from expanding, stress and internal forces develop in the element. That is why the final axial forces are composed of forces caused by mechanical loading and forces caused by thermal expansion.

Consider an example as shown in Figure 23. This example is taken from [12]. The structure consists of three pinned elements. The cross-sectional areas of the elements are respectively 15 cm^2 , 20 cm^2 and 25 cm^2 . Assume $E = 2 \times 10^5 \text{ N/mm}^2$ and $\alpha = 1/75000 \text{ 1/}^\circ\text{C}$.

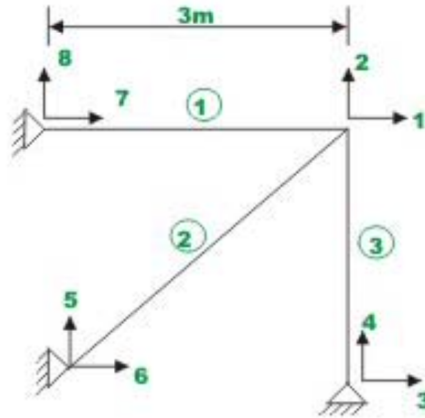


Figure 23 Truss example (taken from [12])

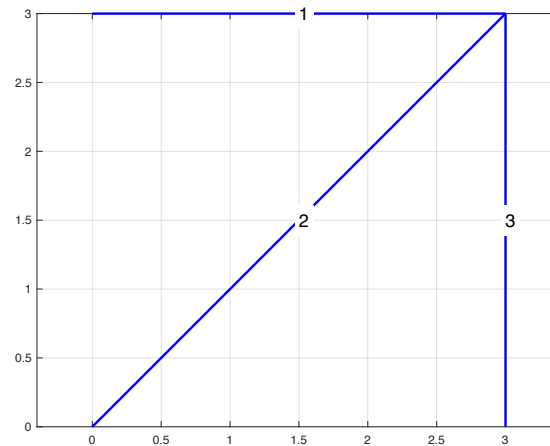


Figure 24 Truss example (created in [18])

Let us assume that the temperature of the element (2) is raised by 40°C .

Due to boundary conditions, it is clear from Figure 23 that the displacements

$$u_3 = u_4 = u_5 = u_6 = u_7 = u_8 = 0.$$

The global stiffness matrix of the size 8×8 is assembled as

$$\mathbf{K} = 10^3 \begin{bmatrix} 147.14 & 47.14 & 0 & 0 & -47.14 & -47.14 & -100 & 0 \\ 47.14 & 147.14 & 0 & -100 & -47.14 & -47.14 & 0 & 0 \\ 0 & 0 & 0 & 0 & 0 & 0 & 0 & 0 \\ 0 & -100 & 0 & 100 & 0 & 0 & 0 & 0 \\ -47.14 & -47.14 & 0 & 0 & 47.14 & 47.14 & 0 & 0 \\ -47.14 & 47.14 & 0 & 0 & 47.14 & 47.14 & 0 & 0 \\ -100 & 0 & 0 & 0 & 0 & 0 & 100 & 0 \\ 0 & 0 & 0 & 0 & 0 & 0 & 0 & 0 \end{bmatrix} \text{ kN/m.} \quad (5.51)$$

and for each element the vector of the forces caused by the heat \mathbf{f}^e is calculated from the equation (5.40).

After the assembly the vector of the heat forces is

$$\mathbf{f}_t = \begin{Bmatrix} -640 \\ -640 \\ 0 \\ 0 \\ 640 \\ 640 \end{Bmatrix} \text{ kN.} \quad (5.52)$$

The unknown displacements u_1 and u_2 are calculated from

$$\mathbf{K}_{11} \mathbf{u} + \mathbf{K}_{12} \mathbf{k} = \mathbf{f} - \mathbf{f}_t. \quad (5.53)$$

from which \mathbf{u} is formularized as

$$\mathbf{u} = \mathbf{K}_{11}^{-1}(\mathbf{f} - \mathbf{f}_t - \mathbf{K}_{12} \mathbf{k}) = \begin{Bmatrix} 0.0033 \\ 0.0033 \end{Bmatrix} \text{ m.} \quad (5.54)$$

The reactions in the supports are then calculated as

$$\mathbf{R} = \mathbf{K}_{21} \mathbf{u} + \mathbf{K}_{22} \mathbf{k} = \begin{Bmatrix} 0 \\ -329.42 \\ 329.42 \\ 329.42 \\ -329.42 \\ 0 \end{Bmatrix} \text{ kN.} \quad (5.55)$$

To calculate the axial force in the element (2) it is firstly necessary to know the elongation of the element. The elongation of the element (2) due to the raised temperature is calculated using the relation

$$dL = \alpha L dT = 0.0023 \text{ m.} \quad (5.56)$$

From the elongation it is possible to finally calculate the axial force in the element (2) as

$$N = E A/L \begin{Bmatrix} -C \\ -S \\ C \\ S \end{Bmatrix} \begin{Bmatrix} u_5 \\ u_6 \\ u_1 \\ u_2 \end{Bmatrix} - E A \frac{dL}{L} = 225.9 \text{ kN.} \quad (5.57)$$

Since the axial force is positive, the element (2) is in tension.

If the temperature of the element (2) was raised by another 40°C to 80°C, the axial force would change to $N = 451.79 \text{ kN}$.

5.3.7 Complex example

Consider a truss as shown in Figure 25.

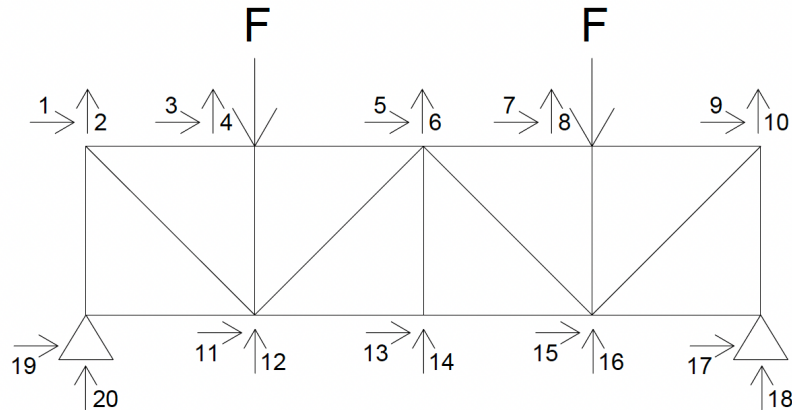


Figure 25 Truss structure

The truss structure comprises 17 elements (bars). The bars are assigned numbers as illustrated in Figure 26.

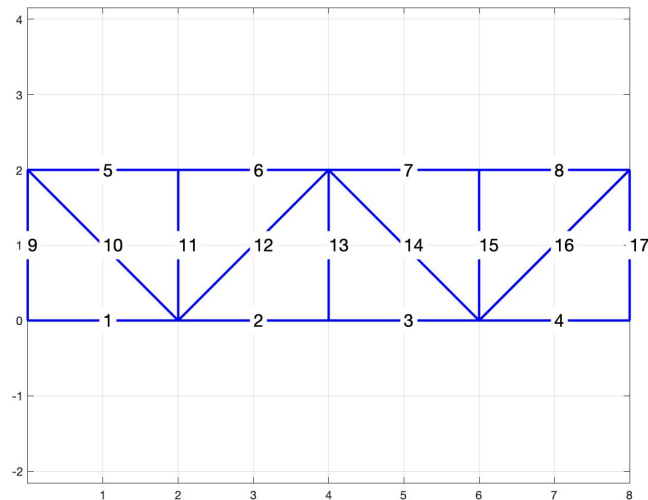


Figure 26 Truss structure (created in [18])

The structure is subjected to two external forces $F = 0.5 \text{ kN}$. Let us assume the modulus of elasticity $E = 30 \times 10^3 \text{ Pa}$ and sectional area of the elements $A = 0.2 \text{ m}^2$. The lower bars (1–4) are subjected to a temperature of 100°C .

From the boundary conditions is clear that the displacements

$$u_{17} = u_{18} = u_{19} = u_{20} = 0. \quad (5.58)$$

Firstly, the global stiffness matrix of the size 20×20 is assembled. Next, the vector of external forces and vector of the heat forces are put together as

$$\mathbf{f} = \begin{Bmatrix} 0 \\ 0 \\ 0 \\ -500 \\ 0 \\ 0 \\ 0 \\ -500 \\ 0 \\ 0 \\ 0 \\ 0 \\ 0 \\ 0 \\ 0 \\ 0 \\ 0 \\ 0 \\ 0 \\ 0 \end{Bmatrix} \text{ N}, \quad \mathbf{f}_t = \begin{Bmatrix} 0 \\ 0 \\ 0 \\ 0 \\ 0 \\ 0 \\ 0 \\ 0 \\ 0 \\ 0 \\ 0 \\ 0 \\ 0 \\ 0 \\ 0 \\ 0 \\ 0 \\ -14.4 \\ 0 \\ 14.4 \\ 0 \end{Bmatrix} \text{ N}. \quad (5.59)$$

Then the unknown displacements u_1 to u_{16} are calculated from (5.53) as

$$\mathbf{u} = \mathbf{K}_{11}(\mathbf{f} - \mathbf{f}_t - \mathbf{K}_{12} \mathbf{k}) = \begin{Bmatrix} 0.333 \\ -0.167 \\ 0.167 \\ -1.221 \\ 0 \\ -1.138 \\ -0.167 \\ -1.221 \\ -0.333 \\ -0.167 \\ -0.083 \\ -1.055 \\ 0 \\ -1.138 \\ 0.083 \\ -1.055 \end{Bmatrix} \text{ m}, \quad (5.60)$$

and from them the reactions as

$$\mathbf{R} = \mathbf{K}_{21} \mathbf{u} + \mathbf{K}_{22} \mathbf{k} = \begin{Bmatrix} -264.4 \\ 500 \\ 264.4 \\ 500 \end{Bmatrix} \text{ N}. \quad (5.61)$$

Let us calculate the axial force in the element (3). The elongation of this element due to the raised temperature is calculated using the relation

$$dL = \alpha L dT = 0.0024 \text{ m.} \tag{5.62}$$

From the elongation it is possible to finally calculate the axial force in the element (2) as

$$N = E A/L \begin{Bmatrix} -C \\ -S \\ C \\ S \end{Bmatrix} \begin{Bmatrix} u_{13} \\ u_{14} \\ u_{15} \\ u_{16} \end{Bmatrix} - E A \frac{dL}{L} = 242.8 \text{ N.} \tag{5.63}$$

The axial force of the element is positive, therefore the element is in tension.

The axial forces of all the elements as well as the displacements shows Figure 27. Elements in tension are in red color, elements in compression in green.

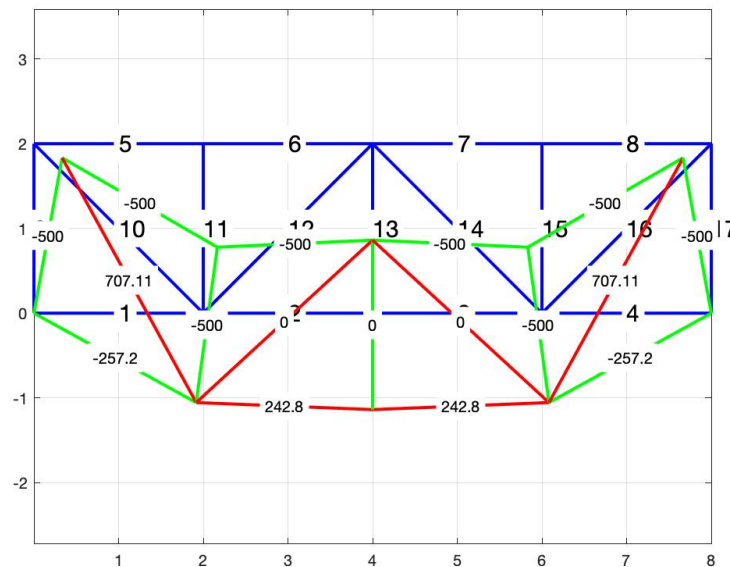


Figure 27 Displacements and axial forces

Now assume that the temperature in the lower bars is raised to 300°C. Figure 28 shows that the axial forces have changed. Higher temperatures result in greater compression and smaller tension of the lower bars.

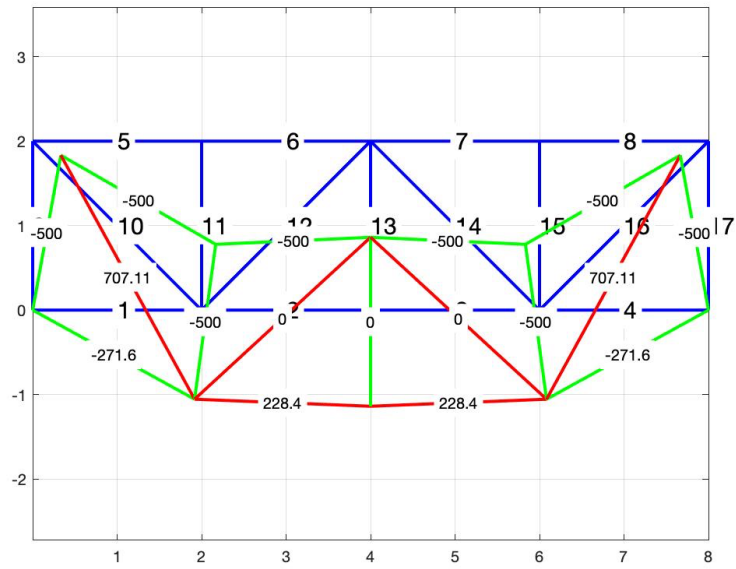


Figure 28 Displacements and axial forces after raising the temperature in the lower bars

For comparison, Figure 29 shows the axial forces in the structure not affected by the thermal loading:

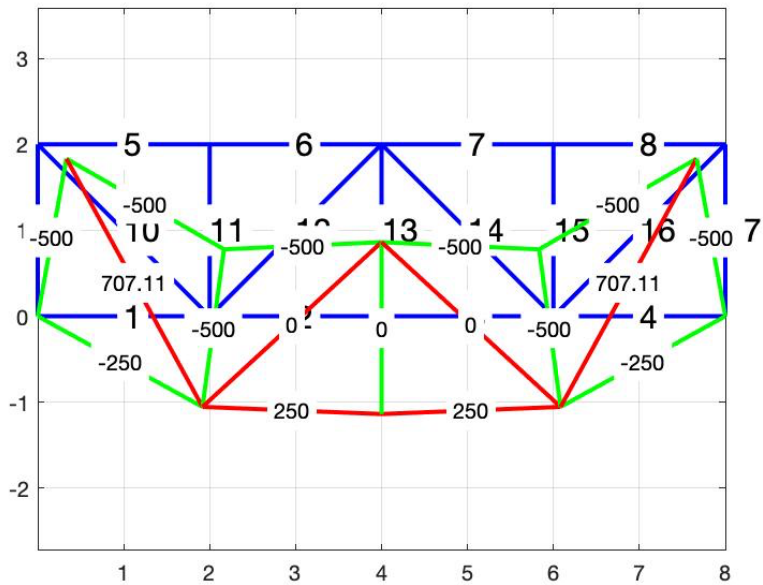


Figure 29 Displacements and axial forces without thermal loading

6 Analysis of a reinforced concrete ceiling slab at normal temperature

The main goal of this thesis is to design an algorithm for analyzing a reinforced concrete slab exposed to thermal loading. The previous chapters dealt with different ways of investigating separately thermal and mechanical behavior of structures, which served as research on possible methods to use in this algorithm. Eventually, we decided for a slightly different approach, which is in detail explained in this chapter. At this point both thermal and mechanical analyses are coupled together for the purpose of analyzing a reinforced concrete ceiling slab.

The algorithm designing process was divided into two parts, the analysis at normal temperature and then the analysis at high temperatures. This chapter covers the first part of the designing process, that is the analysis at normal temperature. The main principles are same for both analyses.

The calculating program developed in this work was coded in MATLAB [18].

The method chosen for the analysis is very similar to the substitute slender reinforced concrete columns method, which is in detail described e.g., in [13].

The main principle of the method is to determine the moment and curvature dependance [13]. The curve is always defined for a constant value of the axial force (see Figure 30). The dependance curve is denoted as κ in Figure 30. According to [14], this method can be successfully used not only in columns analysis, but in a slab analysis as well, provided that the axial force is always set to zero.

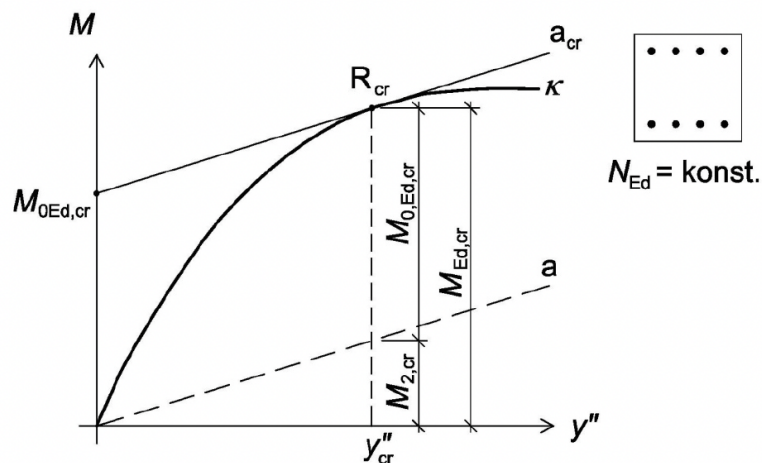


Figure 30 Moment-curvature diagram (taken from [13])

For different curvatures the equilibrium of internal and external forces is calculated. The moment of internal forces calculated to the center of the cross-section is the moment for that precise curvature. After calculating moment for different curvatures and connecting the values, the diagram is drawn. The curve ends, when the limit strain value is reached in at least one of the materials. The maximum moment capacity for the defined cross-section and constant value of the axial force is the maximum moment value in the moment-curvature diagram. This is also the value we are looking for when analyzing the slab.

This method can be used for structures either at normal or at high temperatures. The differences in the method and input parameters are specified in the next chapter.

The concept of the program is following. For different values of curvature, the corresponding height of the compressed part of cross-section is obtained from the equilibrium of internal forces. For each curvature, the corresponding moment capacity is calculated. The program stops once such a curvature is reached, for which the internal forces equilibrium no longer exists. The program then plots the moment-curvature diagram from which the maximum moment capacity for the given cross-section is procured as a maximum moment value of the diagram.

The program is based on the following assumptions:

- Bernoulli-Navier hypothesis before and after deformation,
- the parameters of the cross-section such as geometry and dimensions are known,
- the mechanical and thermal material properties for normal temperatures are known,
- the strain of the reinforcement and the concrete in the same place is assumed to be the same,
- concrete in tension is neglected,
- since the program focuses on purely bent structures, such as slabs, the axial force is always equal to zero.

Amongst the advantages of using this program count:

- although it currently works with material properties as specified in EN 1992-1-1 [15], these can be easily customized,
- the upper reinforcement is optionally included, and the moment capacity is calculated with its addition.

In this chapter each step of the design is described. Part of the design is a verification with existing programs based on several benchmark examples of a slab with given parameters.

6.1 Required inputs

Following inputs are necessary to specify in the algorithm:

Geometry:

- the height of the cross-section h
- the area of the reinforcement in tension A_{s1} and in compression A_{s2}
- the diameter of the reinforcing bars in tension ϕ_{s1} and in compression ϕ_{s2}

Material properties

- concrete characteristic strength f_{ck}
- steel characteristic yield strength f_{yk}
- Young's modulus of elasticity for steel E_s

6.1.1 Material properties at normal temperature

Material properties of both concrete and reinforcing steel are taken from [7]. For concrete, the parabolic-rectangular stress-strain diagram describes the behavior of the material at normal temperatures as illustrated in EN 1992-1-1 [15], Fig. 3.3 (see Figure 31).

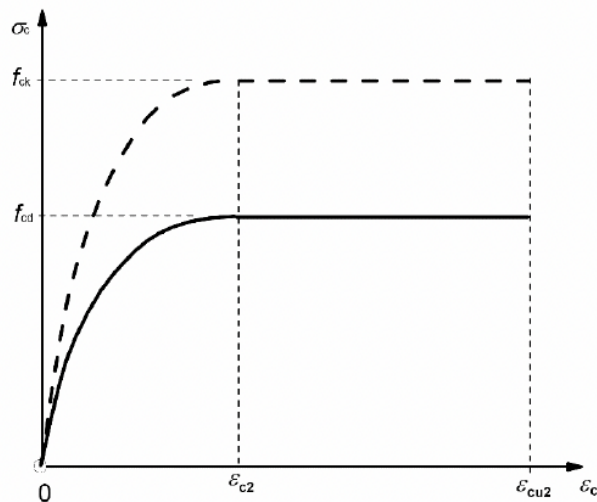


Figure 31 Parabolic-rectangular stress-strain diagram of concrete (taken from [15])

For steel, the bi-linear stress-strain diagram is assumed as illustrated in EN 1992-1-1 [15], Fig. 3.8 (see Figure 32). For the algorithm the diagram with a horizontal top branch is selected.

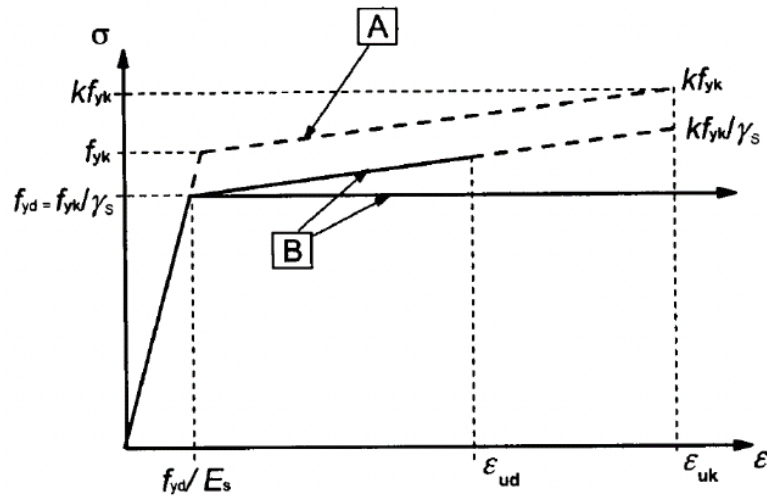


Figure 32 Bi-linear stress-strain diagram of steel (taken from [15])

The design strengths of concrete and steel are calculated with accordance to EN 1992-1-1 [15] as

$$f_{cd} = \frac{f_{ck}}{\gamma_c} \text{ for concrete and} \quad (6.1)$$

$$f_{yd} = \frac{f_{yk}}{\gamma_s} \text{ for steel,} \quad (6.2)$$

where γ_c is the coefficient for concrete ($\gamma_c = 1.5$) and γ_s the coefficient for steel ($\gamma_s = 1.15$).

6.2 Load-bearing capacity at normal temperature

The load-bearing capacity is calculated from the equilibrium of the internal forces

$$F_{s1} + F_{s2} + F_c = 0, \quad (6.3)$$

where F_{s1} and F_{s2} are the forces in the reinforcements in tension and compression respectively, and F_c the force in the compressed concrete.

6.2.1 Forces in reinforcements

The forces in reinforcing steel are calculated as

$$F_{si} = A_{si} \sigma_{si}, \quad (6.4)$$

where A_{si} is the area of reinforcement and σ_{si} the stress in reinforcement determined from the stress-strain diagram of steel.

6.2.2 Forces in concrete

The part of the concrete cross-section which is in tension is neglected. Therefore, only the forces in compressed concrete are part of the balance of internal forces.

The force F_C in the compressed concrete is calculated as follows. The compressed part of the cross-section is divided into a finite number of horizontal sections (strips) of equal heights. For this algorithm a value of 100 sections was chosen. For each section the strain ε_{ci} in the center of the section is determined from the similarity of triangles (see Figure 33). The stress in each section is then obtained from the stress-strain diagram. The force in each section is calculated as

$$F_{ci} = \sigma_{ci} b h_i, \quad (6.5)$$

where b is the width of the section, which is in case of a slab 1 m, and h_i is the height of the section, whereas all the sections are of equal height, that means $h_1 = h_2 = \dots = h_{100}$.

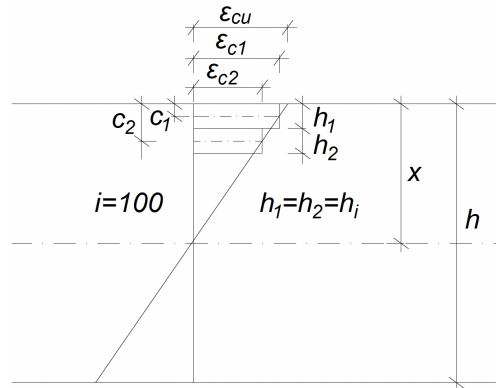


Figure 33 Division of the compressed part of the cross-section into strips

The final force in compressed concrete is then obtained as a sum of forces in the sections

$$\sum_{i=1}^{100} F_{Ci}. \quad (6.6)$$

6.2.3 The load-bearing capacity

The load-bearing capacity of the cross-section is given by the maximum moment capacity M_{Rd} , which is calculated from the internal forces rotating around the center of the cross-section.

Therefore, to determine the load-bearing capacity of the cross-section, the corresponding M_{Rd} is calculated for each curvature. The algorithm starts with a very low value of curvature, for which it finds the equilibrium of internal forces, and subsequently calculates the maximum moment capacity. Then it incrementally adds curvature as

$$y'' = y'' + dy'', \quad (6.7)$$

and repeats the process, as long as the equilibrium can be obtained (see Figure 34).

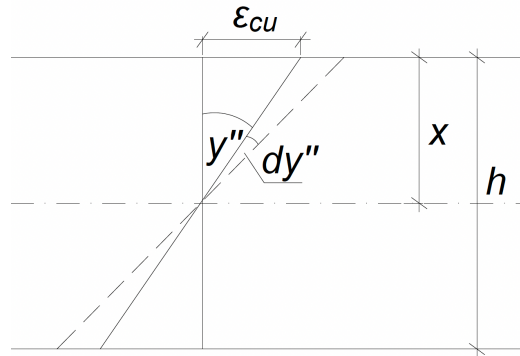


Figure 34 Strain and curvature in the cross-section

Once the program reaches a curvature, for which the internal forces equilibrium does not exist, it plots the moment curvature diagram.

The load-bearing capacity is then given by the maximum value of M_{Rd} in the diagram.

6.3 Methods of determining the height of the compressed part of the cross-section

The easiest way to find the balance between internal forces in the cross-section is to determine a very low value of the height of the compressed part of the cross-section x and gradually increase x in increments dx of a given value (see Figure 35). Amongst the advantages of this method counts simplicity of coding the algorithm. On the other hand, the calculating time of the program is in most cases unnecessarily high.

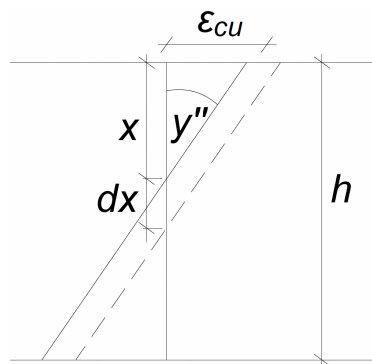


Figure 35 Determining the height of the compressed part of cross-section

Another way of obtaining x is using the interval halving method. The program chooses first x in the middle of the height of the cross-section. If $F_c > F_s$, second x is chosen in the middle of the upper half of the height, if $F_c < F_s$, x is in the middle of the lower half

of the height of the cross-section. Similarly, next x is always chosen in the middle of the previous span, resulting in the new increment being only half as big as the previous one. Using this method, the user can benefit from the calculating time being significantly shorter compared to the previous method.

Even faster and more elegant way of finding x proved to be the following concept. This method is based on the fact, that when x is too small, F_s will always be greater than F_c , which is similar to the previous concept. The algorithm starts with x small enough, that the relation $F_s - F_c > 0$ is true. In each following step an increment is added to x , until finally $F_s - F_c < 0$. At this point, the algorithm linearly interpolates between the x and x from the previous step, from which it obtains a new x , where $F_s - F_c \sim 0$. With this new x obtained from the interpolation the algorithm calculates the difference in the internal forces $F_s - F_c$. This process is repeated until the difference $F_s - F_c$ is smaller than a required value.

In the designed algorithm, the last of the methods of obtaining x was used due to its shortest average calculating time and versatility.

6.4 The description of the algorithm at normal temperature

The algorithm serves as a tool to analyze reinforced concrete slabs.

The algorithm:

1. Entry parameters specification: material properties, geometry
2. Incremental cycle $y'' = 0.005 \rightarrow$ infinite
3. while $R > 1 N$; Residuuum $R = F_c + F_{s1} + F_{s2}$
4. $x = x + dx$ or linear interpolation
5. calculate ε_{cu}
6. determine strain in reinforcement ε_{s1} and ε_{s2} from the similarity of triangles
7. determine stress in reinforcement σ_{s1} and σ_{s2} for ε_{s1} and ε_{s2} with use of the stress-strain diagram
8. calculate F_{s1} and F_{s2} from the stress
9. for $i = 1 \rightarrow 100$; divide the compressed part of the cross-section into 100 sections (strips)
10. determine strain and stress in each section
11. calculate F_{ci} for each section
12. calculate M_{ci} for each section
13. end for
14. calculate F_c as a sum of F_{ci}
15. calculate $R = F_c + F_{s1} + F_{s2}$
16. end while
17. check for limit strain
18. check for the limit height of the compressed part of the cross-section x
19. calculate the moment capacity M_{Rd}
20. $y'' = y'' + dy''$
21. end incremental cycle once the equilibrium can no longer be found
22. plot moment-curvature diagram

1. Entry parameters specification: material properties, geometry

Firstly, it is necessary to specify material characteristic strengths f_{ck} and f_{yk} and the modulus of elasticity for steel E_s . The geometry of the cross-section needs to be specified as well. The algorithm automatically calculates the yield strain of steel ε_y .

2. The curvature loop

The algorithm starts a cycle which calculates the corresponding moment capacity for different curvatures. Before the loop starts, it is necessary to specify values of initial curvature y'' and increment dy'' . The value of increments affects the smoothness of the moment-curvature diagram. For this algorithm the initial curvature as well as value of the increments was set to $y'' = dy'' = 0.005 \text{ m}^{-1}$.

The loop automatically ends once it is no longer possible to reach the equilibrium of the internal forces.

3. While cycle

To calculate the moment capacity for each curvature, the height of the compressed cross-section needs to be determined, for which the equilibrium with the required precision is reached.

Firstly, the required precision needs to be specified. For this algorithm a required precision $R = 1 \text{ N}$ is set.

The height of the compressed part of cross-section is determined with use of the method described in chapter 6.3. For each x in the loop the strain in the upper fibers is calculated as

$$\varepsilon_{cu} = x y'', \tag{6.8}$$

which illustrates Figure 34.

Since the method presumes Bernoulli-Navier behavior before and after deformation, strain in any part of the cross-section can be determined from the similarity of triangles.

With use of the stress-strain diagrams the stresses and then the corresponding internal forces in reinforcements as well as in compressed concrete are calculated. The residuum R is calculated from the forces in reinforcements and concrete as

$$R = F_c + F_{s1} + F_{s2}. \tag{6.9}$$

If the residuum does not meet the criteria for precision, that is if the absolute value of R is greater than the value of the required precision, the height of the compressed part of cross-section x is modified, either by linear interpolation or incrementally.

The loop ends as soon as the criterium for precision is met.

17. Check for limit strain

Once the equilibrium of internal forces is acquired, it is necessary to check the final value of the strain in upper fibers ε_{cu} . If ε_{cu} is smaller than limit strain given in the stress-strain diagram for concrete ε_{cu2} , the algorithm proceeds to a next step. However, if the limit strain is exceeded, the cross-section is above its maximum load-bearing capacity and the calculations are terminated.

18. Check for the limit height of the compressed part of the cross-section x

If $0 < x < h$,

where h is the height of the cross-section, the algorithm proceeds to a next step. Otherwise, if x does not meet the criterium above, the equilibrium of internal forces cannot be found, and the calculations are terminated.

6.5 Verification with existing programs

To find out the correctness and accuracy of the algorithm, two existing computer programs, RCC [19] and InDion [20] were selected to verificate the calculations with use of so-called benchmark examples. Both programs were created by the Department of Concrete and Masonry Structures at CTU in Prague and are available free of charge. RCC [19] is a program for designing reinforced concrete columns. It calculates the moment capacity for a specific cross-section and plots the moment-curvature diagram. InDion [20] is a program which plots interaction diagram of a cross-section based on given parameters, such as geometry and material parameters.

6.5.1 Benchmark example No. 1

Consider a reinforced concrete slab with following parameters:

$h = 200$ mm, $A_{s1} = A_{s2} = 374$ mm², $\phi = 10$ mm, $c = 25$ mm, axial force $N = 0$ kN, concrete C20/25, $f_{yk} = 500$ MPa, $E_s = 200$ GPa

This example is firstly solved with use of the newly designed algorithm. The input to the algorithm with the material properties and geometry is shown in Figure 36.

```

7      %input
8 -    fck = 20; % MPa
9 -    fyk = 500; % MPa
10 -   As1 = 374; % mm2/m
11 -   As2 = 374; % mm2/m
12 -    h = 200; % mm
13 -    c = 25; % mm
14 -   diam_s1 = 10; % mm reinforcement in tension
15 -   diam_s2 = 10; % mm reinforcement in compression
16 -    Es = 200000; % MPa

```

Figure 36 Input in the designed algorithm

Figure 37 shows the output of the algorithm, which takes form of a moment-curvature diagram. As the diagram shows, the maximum moment capacity calculated with use of the design algorithm is $M_{Rd} = 27.79$ kNm.

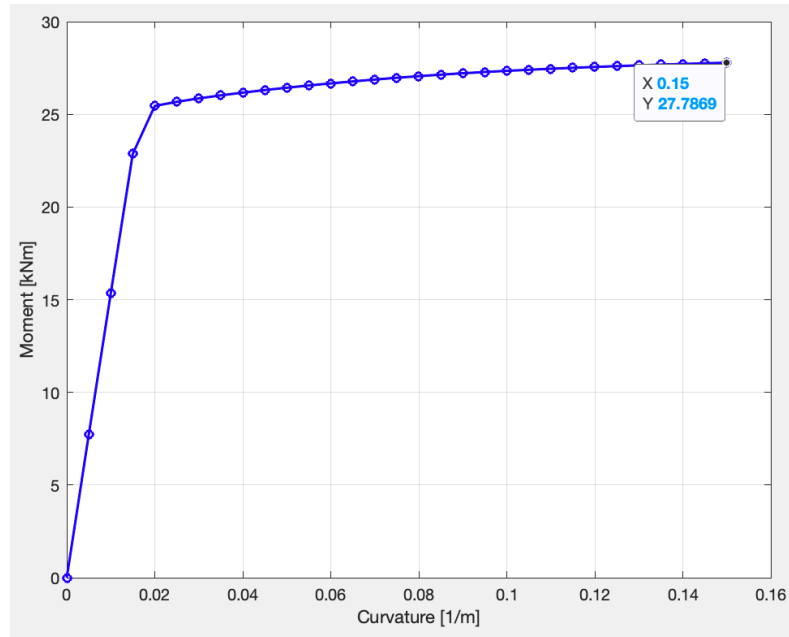


Figure 37 Output from the designed algorithm; moment-curvature diagram

The same example was solved with use of the computer program RCC [19]. Figure 38 shows the preprocessor of RCC [19] with filled-in parameters such as dimensions, load, and materials. Since the program does not allow zero axial force, the axial force $N_{Ed} = 1$ N was inserted instead, which has an insignificant impact on the result. As the program's primary use is for designing columns, the cross-section of the slab is in the preprocessor represented by a width of 1 m.

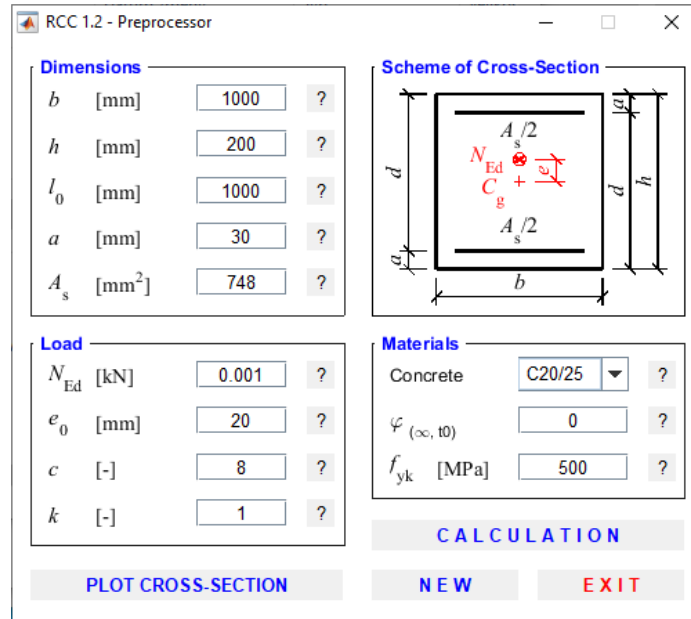


Figure 38 RCC [19] Preprocessor

The output of RCC [19] (Figure 41) takes form of a moment capacity, which is very convenient for the verification with the designed algorithm.

According to RCC [19], $M_{Rd} = 27.7$ kNm, which makes a total difference of 0.09 kNm from the moment calculated with the algorithm.

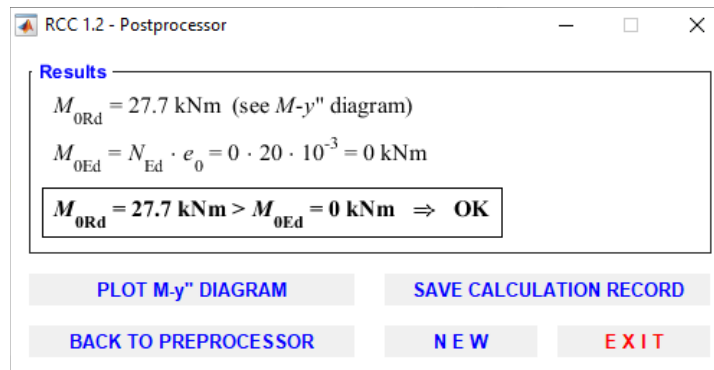


Figure 39 RCC [19] Postprocessor

The same input parameters were then inserted in the computer program InDion [20]. The cross-section of a slab was represented by a cross-section of a width of 1 m as shows Figure 40.

InDiOn - Interakční Diagram Online

Program pro vykreslení interakčního diagramu průřezu

Charakteristiky průřezu

b = mm

h = mm

d₁ = mm

d₂ = mm

A_{s1} = mm²

A_{s2} = mm²

Materiály

f_{ck} = MPa

f_{yk} = MPa

E_s = GPa

Působící vnitřní síly

N_{Ed} = kN

M_{Ed} = kNm

Figure 40 Input in InDion [20]

The output of InDion [20] takes form of an interaction diagram and 6 points of the diagram. For the verification of the algorithm, we were interested in the moment value for an axial force equal to zero (M_{Rd3}), which can be compared to the maximum moment obtained from the algorithm.

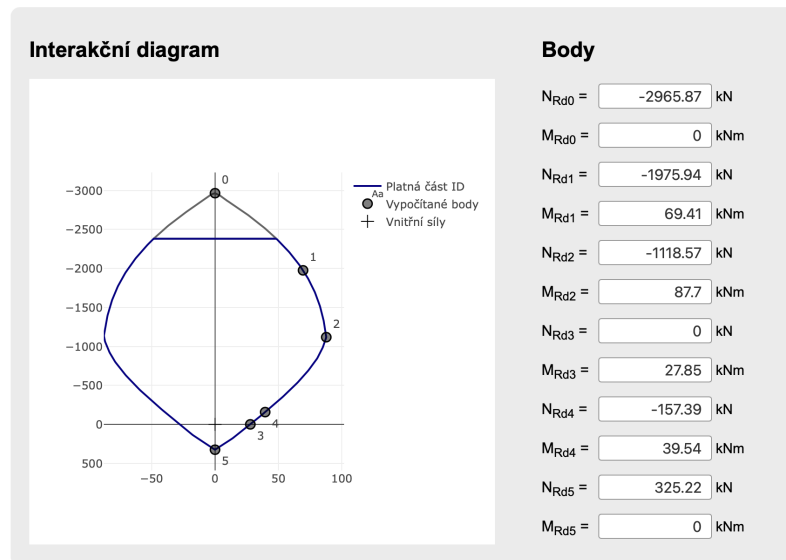


Figure 41 Output from InDion [20]

As shown in Figure 41, the moment capacity for zero axial force calculated in InDion [20] is $M_{Rd3} = 27.85$ kNm.

The total difference between the moments obtained from the designed algorithm and computer program InDion [20] is 0.06 kNm.

6.5.2 Benchmark example No. 2

As a second example, let us assume a reinforced concrete slab with following parameters:

$h = 250$ mm, $A_{s1} = A_{s2} = 1100$ mm², $\phi = 14$ mm, $c = 35$ mm, axial force $N = 0$ kN, concrete C30/37, $f_{yk} = 500$ MPa, $E_s = 200$ GPa

The input parameters in the algorithm are shown in Figure 42.

```

7      %input
8      fck = 30; % MPa
9      fyk = 500; % MPa
10     As1 = 1100; % mm2/m
11     As2 = 1100; % mm2/m
12     h = 250; % mm
13     c = 35; % mm
14     diam_s1 = 14; % mm reinforcement in tension
15     diam_s2 = 14; % mm reinforcement in compression
16     Es = 200000; % MPa
    
```

Figure 42 Input in the designed algorithm

According to the calculations, the maximum moment capacity of the cross-section is $M_{Rd} = 95.24$ kNm (Figure 43).

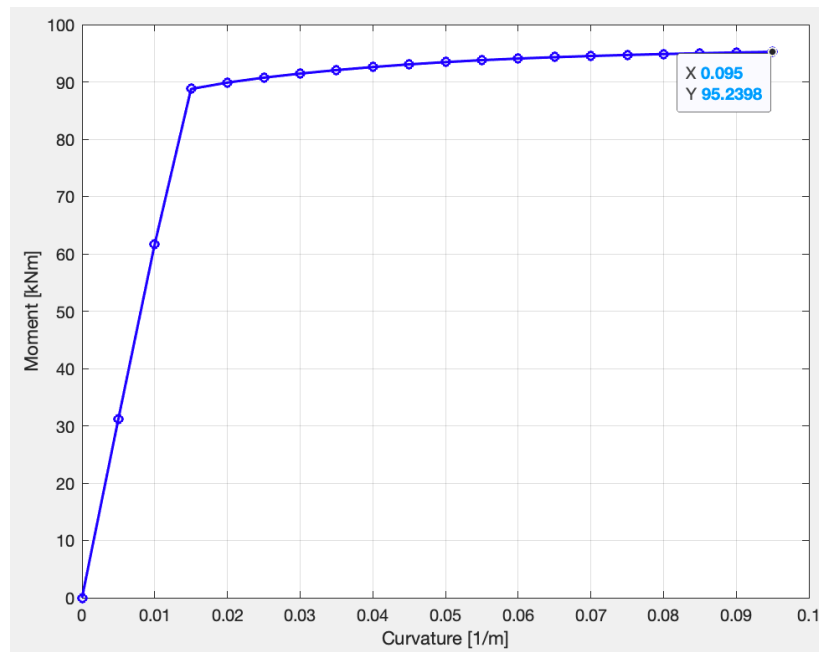


Figure 43 Output from the designed algorithm; moment-curvature diagram

The same example was solved in the computer program RCC [19] as well. The preprocessor and postprocessor of RCC [19] are shown in Figure 44 and Figure 45. According to RCC [19], $M_{Rd} = 94$ kNm, which makes a total difference of 1.24 kNm from the moment capacity calculated with the designed algorithm.

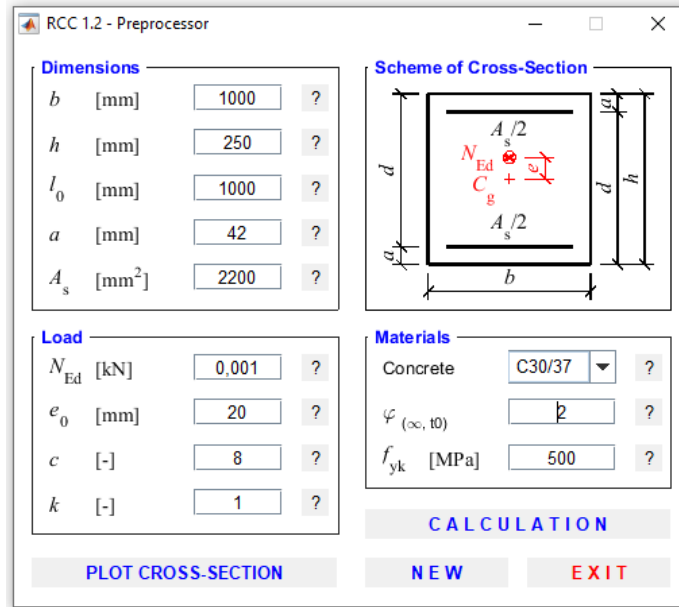


Figure 44 RCC [19] Preprocessor

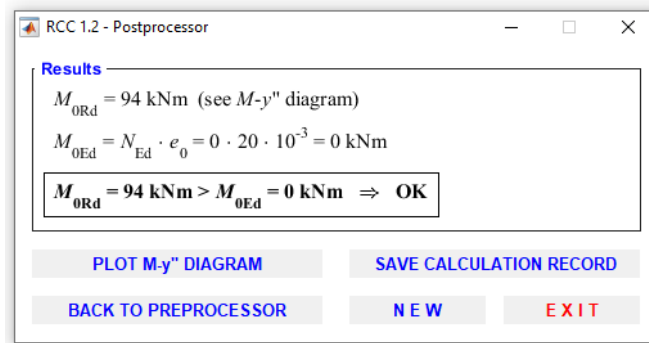


Figure 45 RCC [19] Postprocessor

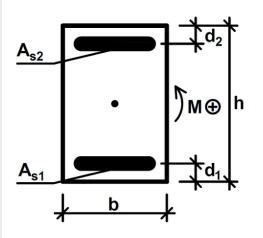
Figure 46 and Figure 47 show the input and output from the computer program InDion [20]. The moment capacity for zero axial force calculated in InDion [20] is $M_{Rd3} = 95.44$ kNm, which compared to the result obtained in the algorithm is 0.2 kNm higher.

InDiOn - Interakční Diagram Online

Program pro vykreslení interakčního diagramu průřezu

Charakteristiky průřezu

$b =$ mm
 $h =$ mm
 $d_1 =$ mm
 $d_2 =$ mm
 $A_{s1} =$ mm²
 $A_{s2} =$ mm²



Materiály

$f_{ck} =$ MPa
 $f_{yk} =$ MPa
 $E_s =$ GPa

Působící vnitřní síly

$N_{Ed} =$ kN
 $M_{Ed} =$ kNm

Figure 46 Input in InDion [20]

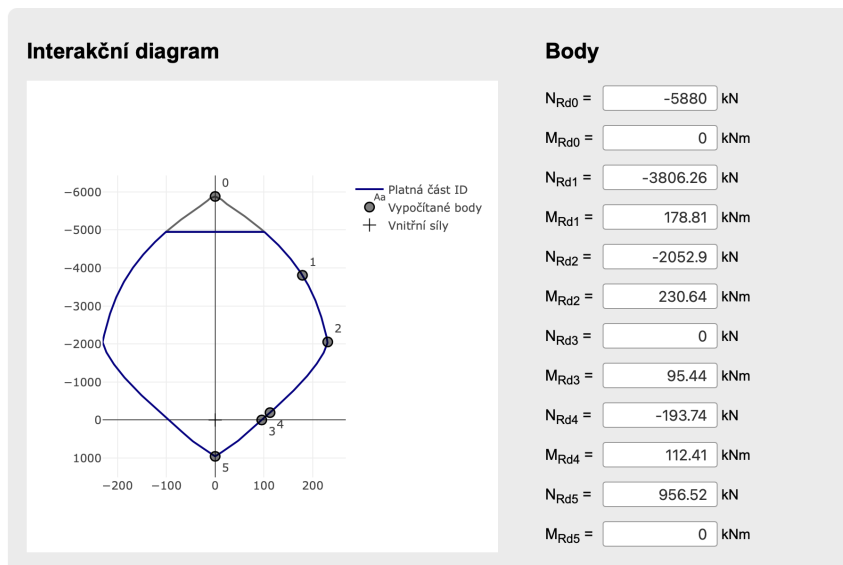


Figure 47 Output from InDion [20]

6.5.3 Benchmark example No. 3

For the third example, let us assume a reinforced concrete slab with following parameters:

$h = 140$ mm, $A_{s1} = 870$ mm², $A_{s2} = 283$ mm², $\phi_1 = 12$ mm, $\phi_2 = 8$ mm, $c = 25$ mm, axial force $N = 0$ kN, concrete C20/25, $f_{yk} = 500$ MPa, $E_s = 200$ GPa

Since the program RCC [19] does not allow different values for A_{s1} and A_{s2} , this example could be verified only with the output from InDion [20].

The input in the algorithm is shown in Figure 48.

```

7      %input
8      fck = 20; % MPa
9      fyk = 500; % MPa
10     As1 = 870; % mm2/m
11     As2 = 283; % mm2/m
12     h = 140; % mm
13     c = 25; % mm
14     diam_s1 = 12; % mm reinforcement in tension
15     diam_s2 = 8; % mm reinforcement in compression
16     Es = 200000; % MPa

```

Figure 48 Input in the designed algorithm

Figure 49 shows the output from the algorithm with the maximum value of the moment capacity $M_{Rd} = 35,69$ kNm.

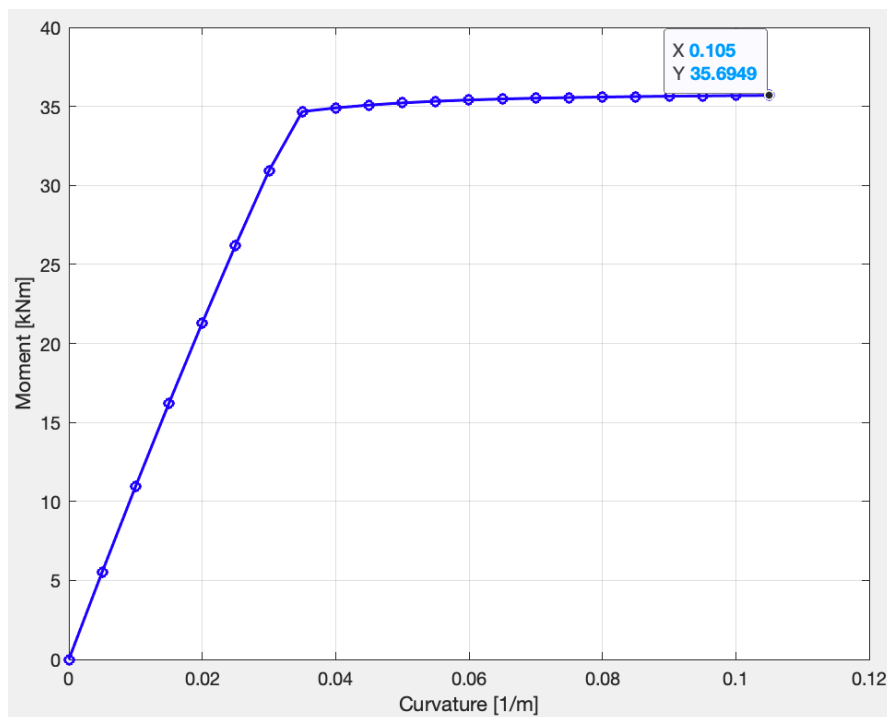


Figure 49 Output from the designed algorithm; moment-curvature diagram

The input in the computer program InDion [20] is shown in Figure 50.

InDiOn - Interakční Diagram Online

Program pro vykreslení interakčního diagramu průřezu

Charakteristiky průřezu

b = mm

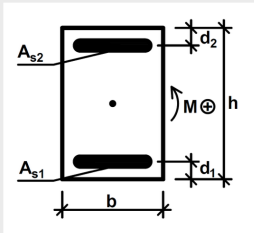
h = mm

d₁ = mm

d₂ = mm

A_{s1} = mm²

A_{s2} = mm²



Materiály

f_{ck} = MPa

f_{yk} = MPa

E_s = GPa

Působící vnitřní síly

N_{Ed} = kN

M_{Ed} = kNm

Figure 50 Input in InDion [20]

As shown in Figure 51, the moment capacity corresponding to zero axial force is $M_{Rd3} = 35.83$ kNm.

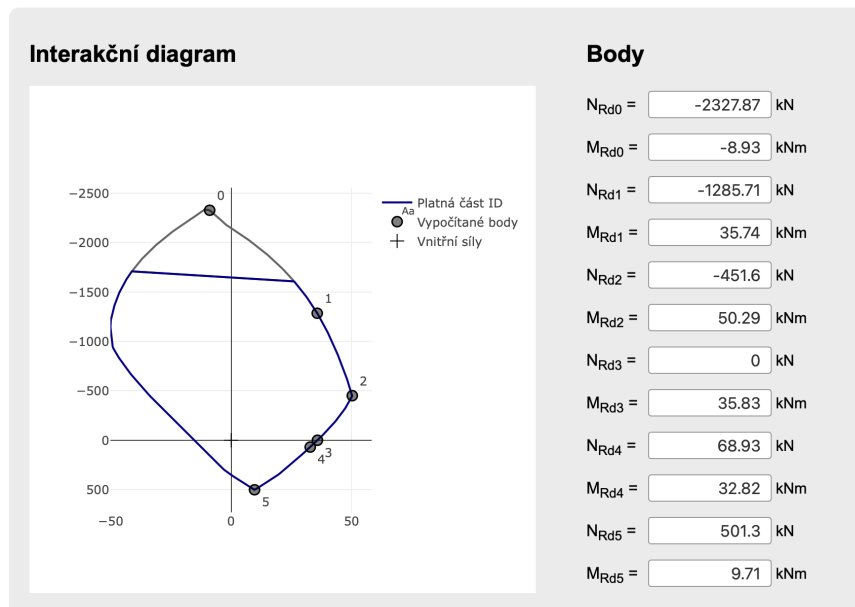


Figure 51 Output from InDion [20]

The total difference between the moments obtained from the designed algorithm and computer program InDion [20] is 0.14 kNm.

6.5.4 Assessment

The differences between the moment values obtained in the designed algorithm and existing programs are in all cases sufficiently small. Therefore, based on the benchmark examples, it can be said that the algorithm works properly with a minimum error and is applicable for a given structure.

7 Analysis of a reinforced concrete ceiling slab at high temperature

The algorithm for the analysis of the reinforced concrete ceiling slab at high temperature has its basis in the algorithm for the analysis at normal temperature, which is in detail described in the previous chapter. Again, for different values of curvature the height of the compressed part of the cross-section is determined from the equilibrium of internal forces. This time, the stress-strain diagrams for materials at high temperatures as specified in EN 1992-1-2 [7] are used. Since the material properties change with temperatures, it is essential to know the temperature of each part of the cross-section at the time step, for which the analysis is performed. The designed algorithm does not include a thermal analysis, instead, it follows up on an existing program TempAnalysis (TA) [17], which focuses on a thermal analysis of a concrete cross-section. The resulting data from TA [17] containing temperatures in the cross section are called in the new algorithm. With this data the algorithm calculates the corresponding moment for each curvature and plots the moment-curvature diagram for the given cross section, from which the maximal moment capacity can be deduced as the greatest moment value.

A pre-requisite for using the algorithm is to have obtained the temperature development of the cross section. The user then specifies parameters such as geometry of the cross-section, material attributes and the required time step.

The program is based on the following assumptions:

- Bernoulli-Navier hypothesis before and after deformation,
- the parameters of the cross-section such as geometry and dimensions are known,
- the mechanical and thermal material properties for normal and high temperatures are known,
- for the high-temperature conditions, the creep and transient strains are neglected,
- concrete in tension is neglected,
- the temperature of the reinforcement is assumed to be equal to the temperature of the concrete in the position of the cross-section, where the center of the rebar is located,
- the strain of the reinforcement and the concrete in the same place is assumed to be the same,
- since the program focuses on purely bent structures, such as slabs, the axial force is always equal to zero.

Amongst the advantages of using this program count:

- the program can be used for any fire model (nominal fire curve, fire curves which include the cooling phase, advanced fire models etc.),
- although it currently works with material properties as specified in EN 1992-1-2 [7], these can be easily customized,
- the upper reinforcement is optionally included, and the moment capacity is calculated with its addition.

7.1 Temperatures in the structure

The program follows up on TempAnalysis [17], a computer program based on FEM for thermal analysis of a cross-section exposed to fire. After entering the geometry of the cross-section, material properties and a fire model in the program, a table of temperatures in each time and location of the cross-section is obtained. For illustration, this table is shown in Figure 52. In the table, the user is given temperatures in 20 seconds time steps and 1 mm thicknesses.

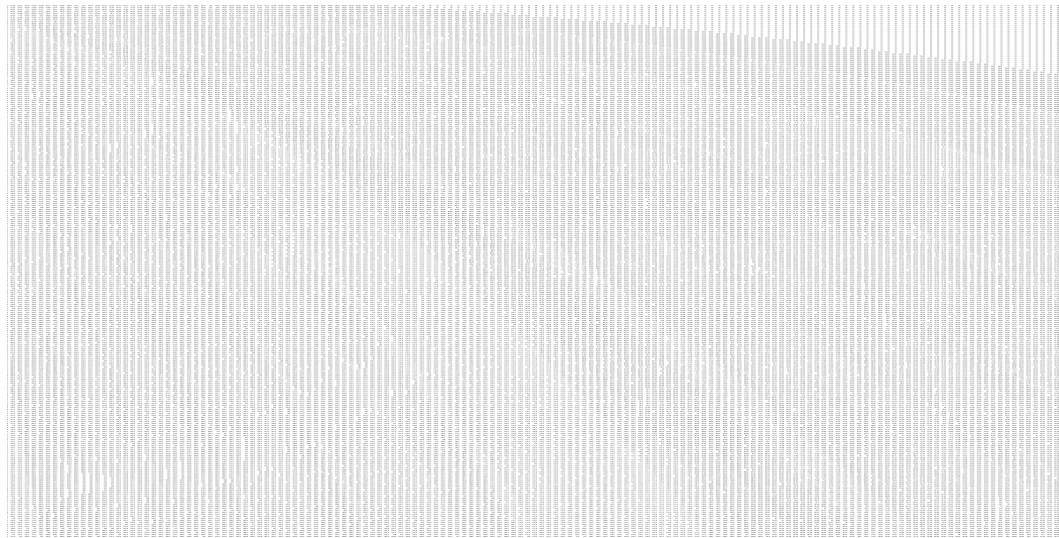


Figure 52 Complete temperature data (obtained from [17])

Notice that the temperatures across the cross-section in the table form isotherm-like shapes similarly to the real thermal development in the structure. This effect is because after zooming out, same numbers look the same.

To do the analysis, it is necessary to be able to define a temperature at any time and location of the cross section including parts and time steps, which are not included in the result table. Therefore, the first step of the program is to do a linear interpolation across the table. For this an independent function was designed, which is later called in the analyzing algorithm.

Three interpolations in total are done to obtain the final temperature at each time step and location. First two interpolate the temperature at the specified height of the cross-section for the closest lower and higher time step. The third interpolation is for the temperature at the specified time step.

For a better understanding, let us assume a slab of a given height $h = 250$ mm, for which a temperature at $x = 21.5$ mm at a time of $t = 3630$ s is to be determined.

Figure 53 shows the TempAnalysis preprocessor, from which the data table is obtained by clicking the button in the bottom-right corner *Save data*.

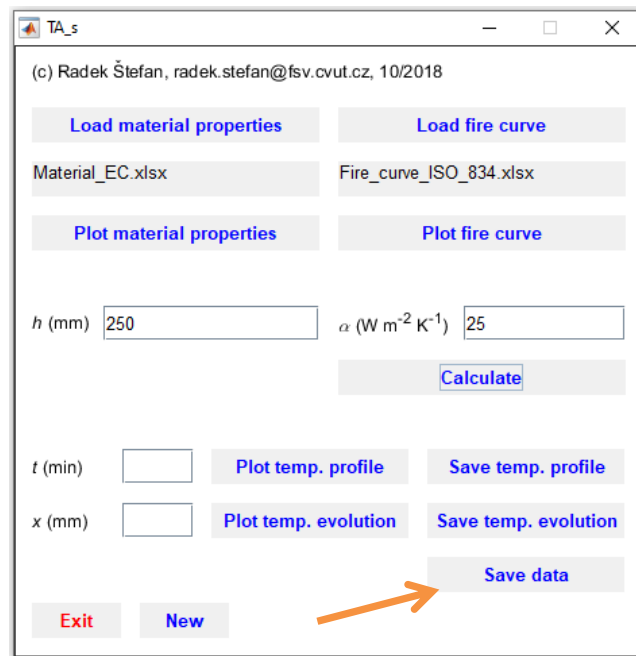


Figure 53 TempAnalysis preprocessor

This table obtains data for time steps of 20 s and thicknesses of whole mm, both starting with a zero. It is clear that the final temperature is located somewhere between the rows 182 and 183 and the columns 22 and 23 and therefore the algorithm will interpolate between the highlighted values in Figure 54.

	U	V	W	X
181	524,2083	511,2185	498,6017	486,3436
182	525,5545	512,5629	499,9436	487,6825
183	526,8933	513,8998	501,2781	489,0141
184	528,2245	515,2293	502,6054	490,3384
185	529,5485	516,5516	503,9254	491,6556

Figure 54 Values used for interpolation

According to a manual linear interpolation, the temperature at $x = 21.5$ mm and time $t = 3630$ s is $\theta = 506.9211^\circ\text{C}$.

To prove the correctness of the manual calculation, let us look at a temperature profile generated from TempAnalysis [17] for time $t = 60$ min = 3600 s, illustrated in Figure 55.

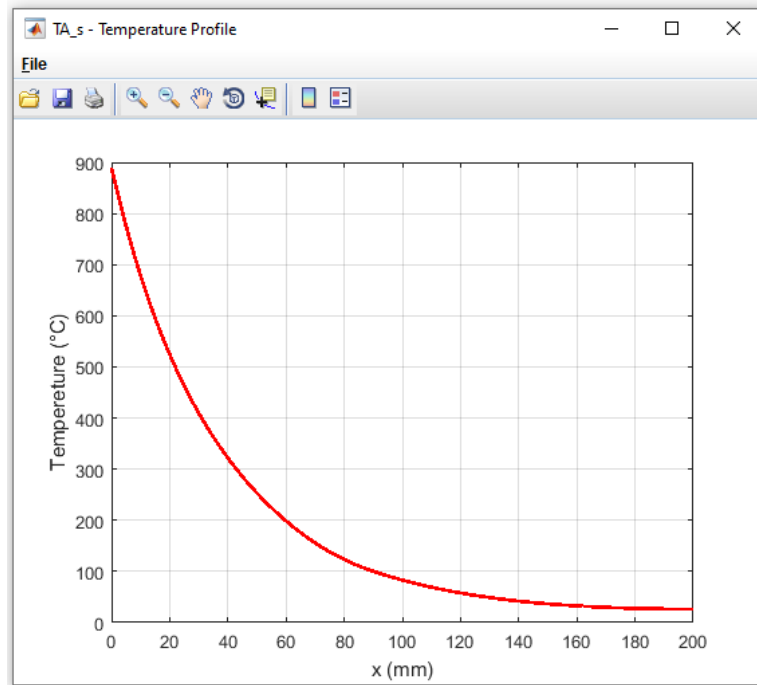


Figure 55 Temperature profile at $t = 60$ min (generated from [17])

According to the temperature profile, the temperature at $x = 21.5$ mm should slightly exceed 500°C .

Now let us enter the required parameters together with the data table in the algorithm as shown in Figure 56.

```

1 - function Temp = f_Interpolate2(Thick, Time)
2 -     Thick = 21.5;
3 -     Time = 3630;
4 -     Matrix = xlsread('Data_ex1');
```

Figure 56 Input in the algorithm for linear interpolation

Based on the input, the algorithm calculates the temperature at $x = 21.5$ mm and time $t = 3630$ s as $\theta = 506.9211^\circ\text{C}$, which is the exact same value as the one obtained from the manual linear interpolation. Therefore, a conclusion can be drawn that the algorithm works correctly.

A boundary condition needed to be specified in case of searching for a temperature at a time step exceeding the range covered in the table. That is why a linear extrapolation is included in the algorithm.

7.2 Load-bearing capacity at high temperatures

A similar approach to the one at normal temperature is employed when calculating the moment-curvature dependence and searching for the maximum load-bearing capacity of the cross-section at high temperatures. However, there are two main differences:

- temperature-dependent material properties of concrete and steel at high temperatures as specified in EN 1992-1-2 [7] are used in the program,
- total strain of both concrete and steel comprises thermal strain and stress-dependent strain.

7.2.1 Material properties at high temperature

The stress-strain diagrams for concrete and steel were changed to correspond with the diagrams described in EN 1992-1-2 [7]. The stress-strain diagram for concrete exposed to high temperatures shown in EN 1992-1-2 [7], Fig. 3.1 is illustrated in Figure 57.

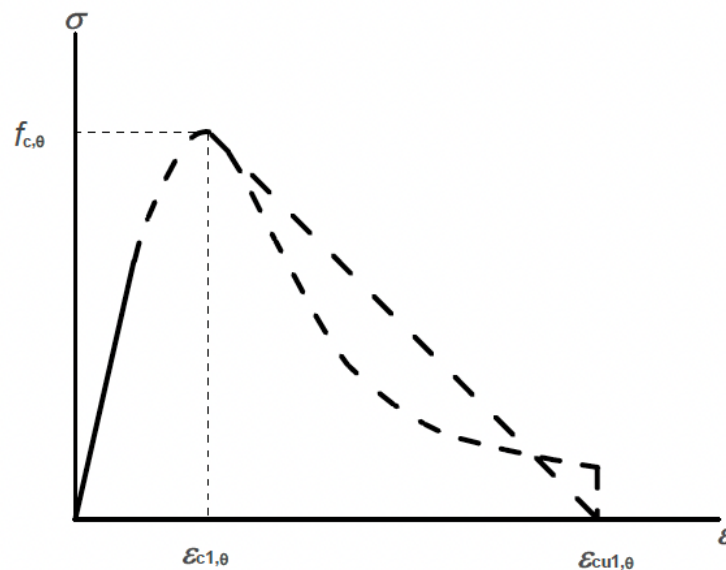


Figure 57 Stress-strain diagram of concrete at high temperatures (taken from [7])

The nonlinear descending curvature is used in the program to achieve a higher accuracy of the calculations. The temperature-dependent parameters of the stress-strain diagram are automatically determined for each temperature from EN 1992-1-2 [7], Table 3.1 (see Figure 58).

Concrete temp. θ	Siliceous aggregates			Calcareous aggregates		
	$f_{c,\theta} / f_{ck}$	$\varepsilon_{c1,\theta}$	$\varepsilon_{cu1,\theta}$	$f_{c,\theta} / f_{ck}$	$\varepsilon_{c1,\theta}$	$\varepsilon_{cu1,\theta}$
[°C]	[-]	[-]	[-]	[-]	[-]	[-]
1	2	3	4	5	6	7
20	1,00	0,0025	0,0200	1,00	0,0025	0,0200
100	1,00	0,0040	0,0225	1,00	0,0040	0,0225
200	0,95	0,0055	0,0250	0,97	0,0055	0,0250
300	0,85	0,0070	0,0275	0,91	0,0070	0,0275
400	0,75	0,0100	0,0300	0,85	0,0100	0,0300
500	0,60	0,0150	0,0325	0,74	0,0150	0,0325
600	0,45	0,0250	0,0350	0,60	0,0250	0,0350
700	0,30	0,0250	0,0375	0,43	0,0250	0,0375
800	0,15	0,0250	0,0400	0,27	0,0250	0,0400
900	0,08	0,0250	0,0425	0,15	0,0250	0,0425
1000	0,04	0,0250	0,0450	0,06	0,0250	0,0450
1100	0,01	0,0250	0,0475	0,02	0,0250	0,0475
1200	0,00	-	-	0,00	-	-

Figure 58 Values for the parameters of the stress-strain relationship of concrete (taken from [7])

The main parameters of the stress-strain diagram of concrete used in the program are those for siliceous aggregates, because of their worse properties compared to the calcareous aggregates, resulting in the algorithm being on the safe side.

The stress-strain diagram for steel exposed to high temperatures shown in EN 1992-1-2 [7], Fig. 3.3 is used in the algorithm. The diagram is illustrated in Figure 59.

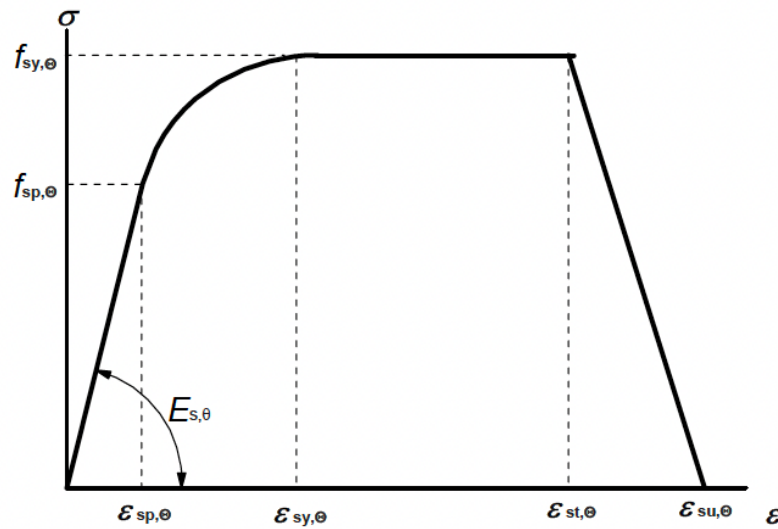


Figure 59 Stress-strain diagram of steel at high temperatures (taken from [7])

The temperature-dependent parameters of the stress-strain diagram are determined for each temperature from EN 1992-1-2 [7], Table 3.2a (see Figure 60).

Steel Temperature θ [°C]	$f_{sy,\theta} / f_{yk}$		$f_{sp,\theta} / f_{yk}$		$E_{s,\theta} / E_s$	
	hot rolled	cold worked	hot rolled	cold worked	hot rolled	cold worked
1	2	3	4	5	6	7
20	1,00	1,00	1,00	1,00	1,00	1,00
100	1,00	1,00	1,00	0,96	1,00	1,00
200	1,00	1,00	0,81	0,92	0,90	0,87
300	1,00	1,00	0,61	0,81	0,80	0,72
400	1,00	0,94	0,42	0,63	0,70	0,56
500	0,78	0,67	0,36	0,44	0,60	0,40
600	0,47	0,40	0,18	0,26	0,31	0,24
700	0,23	0,12	0,07	0,08	0,13	0,08
800	0,11	0,11	0,05	0,06	0,09	0,06
900	0,06	0,08	0,04	0,05	0,07	0,05
1000	0,04	0,05	0,02	0,03	0,04	0,03
1100	0,02	0,03	0,01	0,02	0,02	0,02
1200	0,00	0,00	0,00	0,00	0,00	0,00

Figure 60 Values for the parameters of the stress-strain relationship of steel (taken from [7])

The algorithm works with parameters for hot rolled steel, so only columns number 2, 4 and 6 are included in the code.

The total strain of both concrete and steel at high temperatures is generally assumed to be composed of four strain components (see below). The stress-dependent strain, the thermal strain, the creep strain, and the transient strain [2].

7.2.2 Strain

When analyzing concrete at high temperatures, several material models can be implied, as described in EN 1992-1-2 [7] (see also [2]). In some of the models, the creep strain and the transient strain are implicitly included, in others neglected, as it is stated in EN 1992-1-2 [7] and in [2]. For this work, we chose to neglect the creep strain and the transient strain due to their low impact on the analysis result. Therefore, the total strain is calculated from

$$\varepsilon = \varepsilon_{th} + \varepsilon_{m,c}, \quad (7.1)$$

where ε_{th} is the thermal strain and $\varepsilon_{m,c}$ the stress-dependent strain. The thermal strain of concrete is obtained for each temperature from the diagram illustrated in EN 1992-1-2 [7], Fig. 3.5 (see Figure 61).

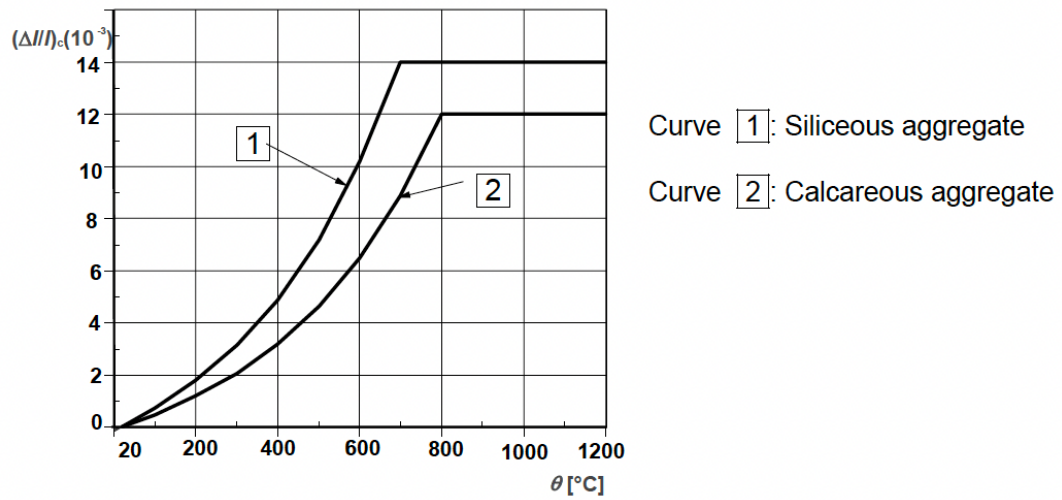


Figure 61 Total thermal elongation of concrete (taken from [7])

When determining the thermal strain, again, the diagram for siliceous aggregates (curve 1) is used in the algorithm.

When analyzing steel under high temperatures, we also follow the simplified approach of neglecting creep strain and transient strain, leading in total steel strain being calculated from

$$\varepsilon = \varepsilon_{th} + \varepsilon_{m,s}, \quad (7.2)$$

where ε_{th} is the thermal strain and $\varepsilon_{m,s}$ the stress-dependent strain. The thermal strain of steel is obtained for each temperature from the diagram illustrated in EN 1992-1-2 [7], Fig. 3.8 (see Figure 62) for reinforcing steel (curve 1).

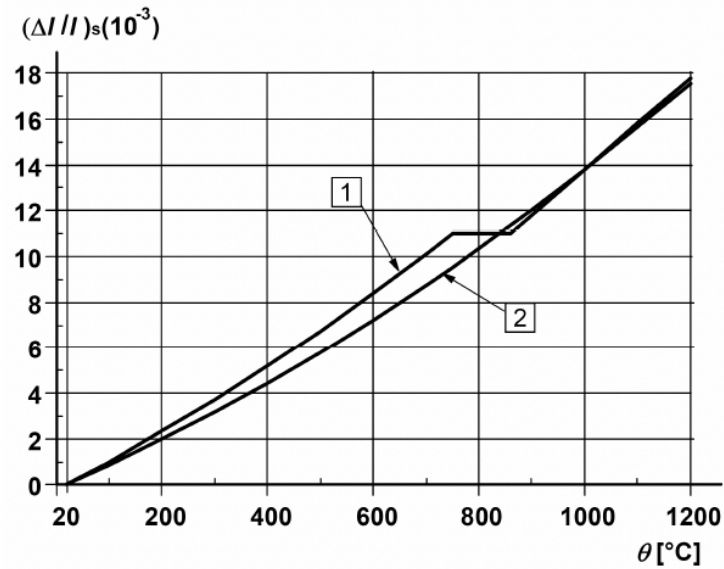


Figure 62 Total thermal elongation of steel (taken from [7])

According to [16], the incorporation of the strain ε_{th} for both concrete and steel in the calculations does not influence the value of the maximum moment capacity M_{Rd} , only the shape of the moment-curvature diagram. Also, since many of the simplified methods of analyzing structures at high temperatures such as the 500°C isotherm or the zone method neglect the thermal strain completely, and assume that

$$\varepsilon = \varepsilon_m, \quad (7.3)$$

when developing the algorithm, the thermal strain ε_{th} was not included in the first calculations and was only added later in accordance with EN 1992-1-2 [7]. The influence of the thermal strain ε_{th} on the output is illustrated in Figure 63.

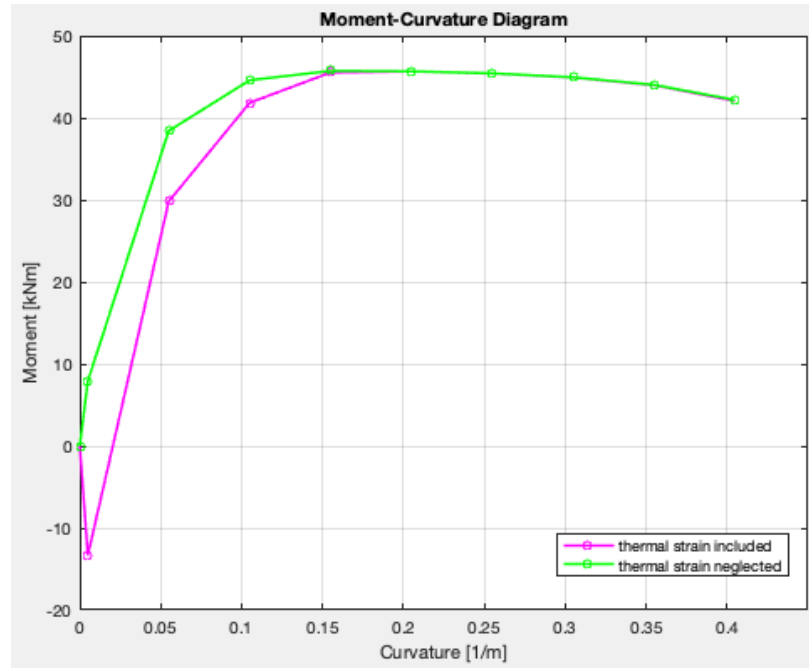


Figure 63 Illustration of the thermal strain effect on the output (created in [18])

From this diagram it is clear, that the thermal strain ε_{th} has in fact no effect on the maximum value of the moment capacity. Instead, it only influences the shape of the moment-curvature diagram. The conclusion drawn here corresponds to [16] and it proves that the basis of the simplified methods in which the thermal strain is neglected does not compromise the accuracy of those methods.

Notice that moment gets into negative values for small values of curvature, which is due to the fact, that in the equation

$$\varepsilon_m = \varepsilon - \varepsilon_{th}, \quad (7.4)$$

thermal strain ε_{th} exceeds the total strain ε . The negative value of ε_m then enters in the stress-strain diagrams to obtain internal stresses and forces in the cross-section.

7.2.3 The description of the algorithm at high temperature

The algorithm serves as a tool to analyze reinforced concrete slabs exposed to high temperatures.

The differences from the previous algorithm for analysis at normal temperature are **highlighted**.

Every time a temperature in the cross-section needs to be obtained from the data table generated from TempAnalysis [17], the algorithm calls the function for linear interpolation, which is described in detail in chapter 7.1.

The algorithm:

1. Entry parameters specification: material properties, geometry, **time step, data from thermal analysis**
2. Incremental cycle $y'' = 0.005 \rightarrow$ infinite
3. while $R > 1 N$; Residuuum $R = F_c + F_{s1} + F_{s2}$
4. $x = x + dx$ or linear interpolation
5. calculate ε_{cu}
6. determine strain in reinforcement ε_{s1} and ε_{s2} from the similarity of triangles
7. **determine $\varepsilon_{th,s}$ and calculate $\varepsilon_{\sigma,m,s}$ as $\varepsilon_{\sigma,m,i,s} = \varepsilon_{si} - \varepsilon_{th,s}$**
8. **determine stress in reinforcement σ_{s1} and σ_{s2} for $\varepsilon_{\sigma,m,1}$ and $\varepsilon_{\sigma,m,2}$ with use of the stress-strain diagram**
9. calculate F_{s1} and F_{s2} from the stress
10. for $i = 1 \rightarrow 100$; divide the compressed part of the cross-section into 100 sections (strips)
11. determine strain in each section ε_{ci} from the similarity of triangles
12. **determine $\varepsilon_{th,ci}$**
13. **calculate $\varepsilon_{\sigma,m,ci}$ as $\varepsilon_{\sigma,m,ci} = \varepsilon_{ci} - \varepsilon_{th,ci}$**
14. **determine stress in each section σ_{ci} for $\varepsilon_{\sigma,m,ci}$ with use of the stress-strain diagram**
15. calculate F_{ci} for each section
16. calculate M_{ci} for each section
17. end for
18. calculate F_c as a sum of F_{ci}
19. calculate $R = F_c + F_{s1} + F_{s2}$
20. end while
21. check for limit strain
22. check for the limit height of the compressed part of the cross-section x
23. calculate the moment capacity M_{Rd}
24. $y'' = y'' + dy''$
25. end incremental cycle once the equilibrium can no longer be found
26. plot moment-curvature diagram

1. Entry parameters specification: material properties, geometry, time step, data from thermal analysis

Firstly, it is necessary to specify material characteristic strengths f_{ck} and f_{yk} and the modulus of elasticity for steel E_s . The geometry of the cross-section needs to be specified as well. The algorithm automatically calculates the yield strain of steel ε_y .

2. The curvature loop

The algorithm starts a cycle which calculates the corresponding moment capacity for different curvatures. Before the loop starts, it is necessary to specify the values of initial curvature y'' and increment dy'' . The value of increments affects the smoothness of the moment-curvature diagram. For this algorithm the initial curvature as well as the value of the increments is set to $y'' = dy'' = 0.005 \text{ m}^{-1}$.

The loop automatically ends once it is no longer possible to reach the equilibrium of the internal forces.

3. While cycle

To calculate the moment capacity for each curvature, the height of the compressed part of cross-section needs to be determined, for which the equilibrium with required precision is reached.

Firstly, the required precision needs to be specified. For this algorithm a required precision $R = 1 \text{ N}$ is set.

The height of the compressed part of cross-section is determined with use of the method described in chapter 6.3. For each x in the loop the strain in the upper fibers is calculated using the relation (6.8).

Since the method presumes Bernoulli-Navier behavior before and after deformation, strain in any part of the cross-section can be determined from the similarity of triangles.

With use of the stress-strain diagrams the stresses and then the corresponding internal forces in reinforcements as well as in compressed concrete are calculated. The residuum R is calculated from the forces in reinforcements and concrete using the equation (6.9).

If the residuum does not meet the criteria for precision, that is if the absolute value of R is greater than the value of the required precision, the height of the compressed part of cross-section x is modified, either by linear interpolation or incrementally.

The loop ends as soon as the criterium for the precision is met.

17. Check for limit strain

Once the equilibrium of internal forces is acquired, it is necessary to check the final value of the strain in upper fibers ε_{cu} . If ε_{cu} is smaller than limit strain given in the stress-strain diagram of concrete ε_{cu2} , the algorithm proceeds to a next step. However, if the limit strain is exceeded, the cross-section is above its maximum load-bearing capacity and the calculations are terminated.

18. Check for the limit height of the compressed part of the cross-section x

If $0 < x < h$,

where h is the height of the cross-section, the algorithm proceeds to the next step. Otherwise, if x does not meet the criterium above, the equilibrium of internal forces cannot be found, and the calculations are terminated.

7.2.4 The effect of high temperatures on load-bearing capacity

To gain an idea on how much the thermal loading influences the load-bearing capacity of the cross-section, let us assume a reinforced concrete slab with following parameters:

$h = 200 \text{ mm}$, $A_{s1} = 714 \text{ mm}^2$, $A_{s2} = 0 \text{ mm}^2$, $\phi_{s1} = 10 \text{ mm}$, $c = 25 \text{ mm}$, axial force $N = 0 \text{ kN}$, concrete C20/25, $f_{yk} = 500 \text{ MPa}$, $E_s = 200 \text{ GPa}$

The slab is exposed to the standard fire curve ISO 834 defined in EN 1991-1-2 [6]. To get an idea of the temperature changes in the cross-section, Figure 64 shows the temperature development in the center of the reinforcing bars. According to the diagram, the temperature in the reinforcement rises from 20°C to almost 600°C in 120 minutes.

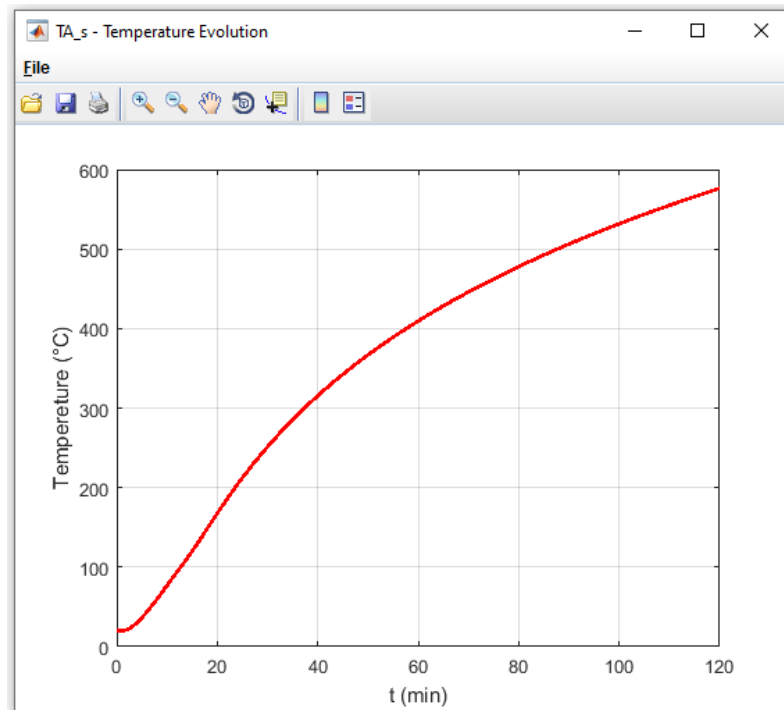


Figure 64 Temperature development at $x = 30 \text{ mm}$ (generated from [17])

The concrete slab and its load-bearing capacity was determined every 20 minutes in a time span of 120 minutes during the exposure to standard fire curve ISO 834 defined in EN 1991-1-2 [6]. For illustration, Figure 65 shows the changes of the moment-curvature dependency in each time step as calculated by the designed algorithm. The maximum moment capacity decreases from the initial value of almost 60 kNm at $t = 0 \text{ min}$ to approximately half its value at $t = 120 \text{ min}$.

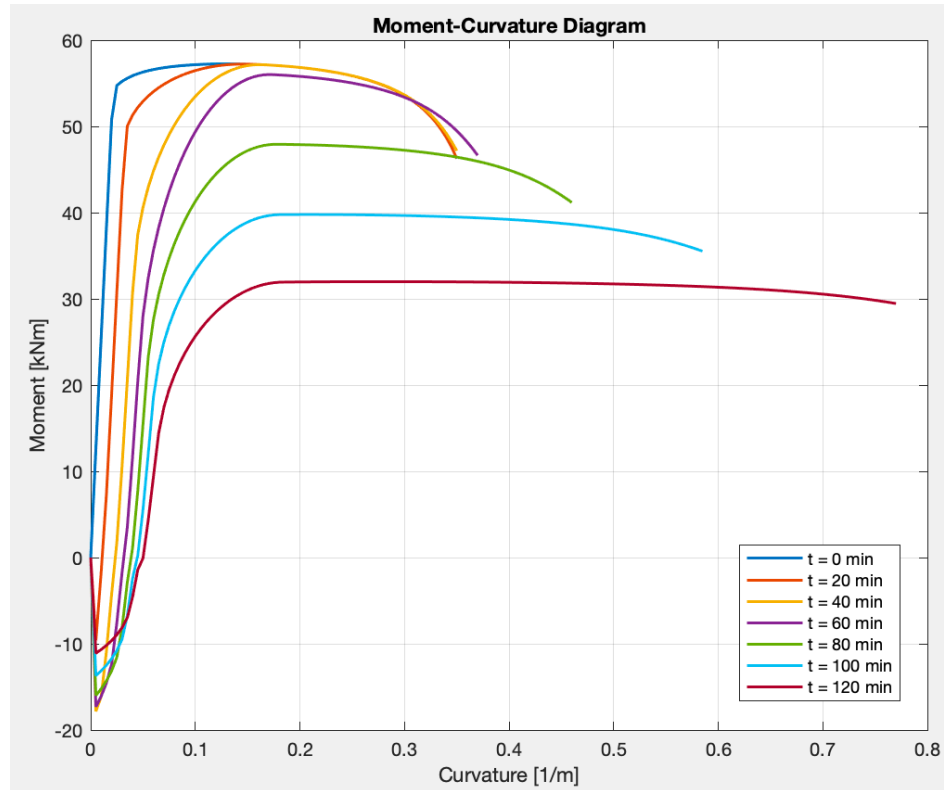


Figure 65 Comparison of moment-curvature diagrams for different times (created in [18])

7.3 Verification with existing methods

To find out the correctness and accuracy of the algorithm, the 500°C isotherm method was selected to verificate the calculations with use of benchmark examples. The method is in detail described in chapter 3.2.1.

The thermal analyses prior to both calculations are done in the computer program TempAnalysis [17].

7.3.1 Benchmark example No. 1

Consider a reinforced concrete slab with following parameters:

$h = 200 \text{ mm}$, $A_{s1} = 655 \text{ mm}^2$, $A_{s2} = 0 \text{ mm}^2$, $\phi_{s1} = 10 \text{ mm}$, $c = 25 \text{ mm}$, axial force $N = 0 \text{ kN}$, concrete C20/25, $f_{yk} = 500 \text{ MPa}$, $E_s = 200 \text{ GPa}$

The slab is subjected to fire, which is in this case represented by the Isotherm 834 curve defined in EN 1991-1-2 [6]. $M_{Rd} = ?$ at time $t = 60 \text{ min}$.

Firstly, the temperatures in the structure are calculated in TempAnalysis [17]. The data from this program are used in both methods. The preprocessor of TempAnalysis [17] is shown in Figure 66.

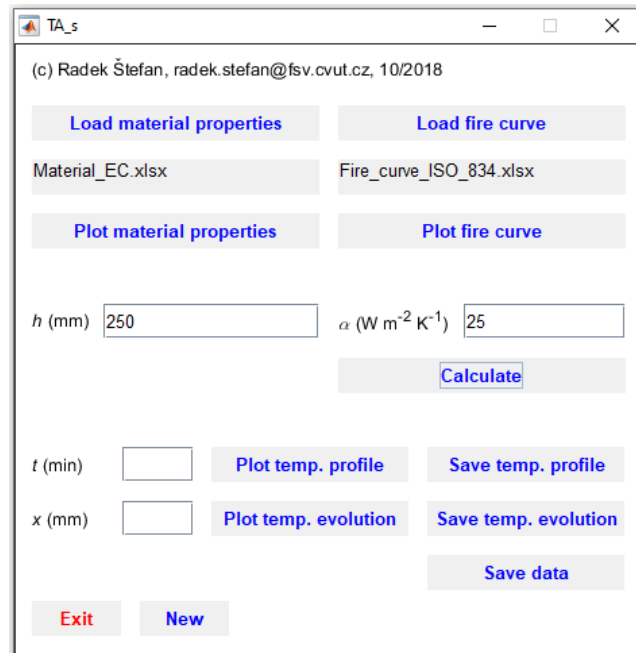


Figure 66 TempAnalysis [17] preprocessor

This example is firstly solved with use of the newly designed algorithm. The input to the algorithm with the material properties and geometry is shown in Figure 67.

```

7   %input
8   -   fyk = 500; % MPa
9   -   fck = 20; % MPa
10  -   As1 = 403; % mm2/m
11  -   As2 = 0; % mm2/m
12  -   h = 200; % mm
13  -   c = 25; % mm
14  -   diam_s1 = 10; % mm lower
15  -   diam_s2 = 0; % mm upper
16  -   Es = 200000; % MPa
17
18  -   Time = 3600; % s
19
20  -   fyd = fyk / 1.15; % MPa
21  -   fcd = fck / 1.5; % MPa
    
```

Figure 67 Input in the designed algorithm

To use the designed algorithm, it is necessary to download the full temperature data from TempAnalysis [17], which are generated in .xls format. The table is added to the code via *xlsread* MATLAB function.

The output of the algorithm shows Figure 68. According to the calculations, the maximum moment capacity of the cross-section at $t = 60$ min is $M_{Rd} = 67.77$ kNm.

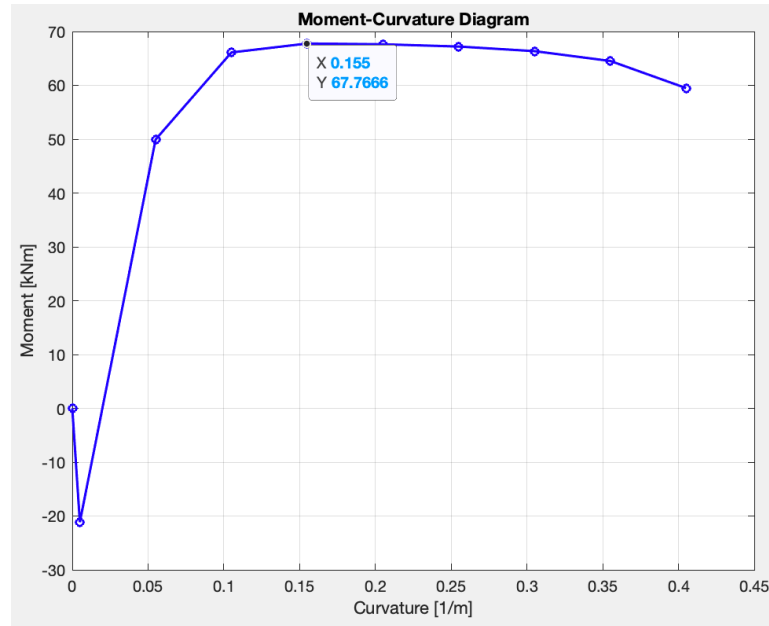


Figure 68 Output from the designed algorithm; moment-curvature diagram

To solve the example with 500°C isotherm method, the temperature profile of the structure at defined time is needed (as shown in Figure 69).

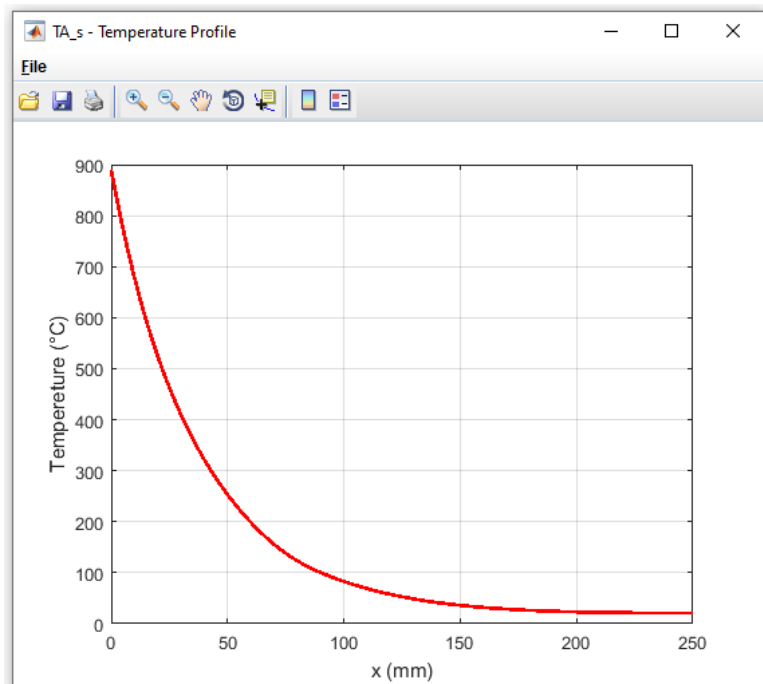


Figure 69 Temperature profile at $t = 60$ min (generated from [17])

From the temperature profile it is clear that the temperature of 500°C is reached at $a_{500} = 23$ mm. The temperature in the center of reinforcing rebars at $a = 30$ mm is $\theta = 410$ °C. This data is sufficient for the 500°C isotherm method, which is shown in use in Table 1.

Table 1 Calculation with use of 500°C isotherm method

	h	=	250	mm		
	a_{500}	=	23	mm		
	h_{fi}	=	$h - a_{500}$	=	227	mm
reinforcement	θ_s	=	410	°C		
	$f_{syd,fi}$	=	$k_{s,fi} f_{yk}$	=	490	MPa
	$k_{s,fi}$	=	0.98			
	A_s	=	655	mm ²		
concrete	$f_{cd,fi}$	=	$f_{ck} / \gamma_{C,fi}$	=	20	MPa
	$\gamma_{C,fi}$	=	1			
	$\gamma_{S,fi}$	=	1			
	γ_M	=	1			
	x	=	$A_s f_{yd} / (0.8 b f_{cd})$	=	26.78	mm
	d	=	$h - c - \phi / 2$	=	220	mm
	z	=	$d - 0.4 x$	=	209.29	mm
	$M_{Rd,fi}$	=	$A_s f_{sy,fi} z / \gamma_{S,fi}$	=	67.17	kNm

According to the 500°C isotherm method, the maximum moment capacity of the cross-section at $t = 60$ min is $M_{Rd} = 67.17$ kNm, which makes a total difference of 0.6 kNm from the moment calculated with the designed algorithm.

7.3.2 Benchmark example No. 2

Consider a reinforced concrete slab with following parameters:

$h = 180$ mm, $A_{s1} = 437$ mm², $A_{s2} = 0$ mm², $\phi_{s1} = 8$ mm, $c = 25$ mm, axial force $N = 0$ kN, concrete C30/37, $f_{yk} = 500$ MPa, $E_s = 200$ GPa

The slab is subjected to fire, which is in this case represented by the Isotherm 834 curve defined in EN 1991-1-2 [6]. $M_{Rd} = ?$ at time $t = 75$ min.

The temperatures in the structure are calculated in TempAnalysis [17]. The preprocessor of TempAnalysis [17] is shown in Figure 70.

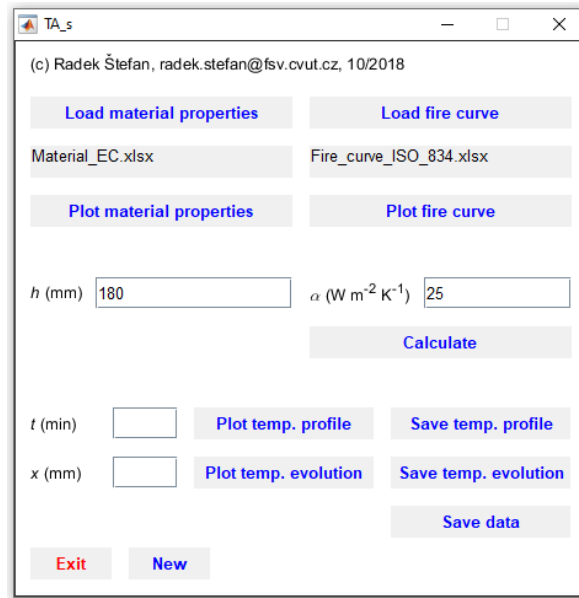


Figure 70 TempAnalysis [17] preprocessor

The input to the algorithm with the material properties and geometry is shown in Figure 71.

```

7      %input
8 -    fyk = 500; % MPa
9 -    fck = 30; % MPa
10 -   As1 = 437; % mm2/m
11 -   As2 = 0; % mm2/m
12 -   h = 180; % mm
13 -   c = 25; % mm
14 -   diam_s1 = 8; % mm lower
15 -   diam_s2 = 0; % mm upper
16 -   Es = 200000; % MPa
17
18 -   Time = 4500; % s
    
```

Figure 71 Input in the designed algorithm

The output of the algorithm shows Figure 72. According to the calculations, the maximum moment capacity of the cross-section at $t = 60$ min is $M_{Rd} = 27.11$ kNm.

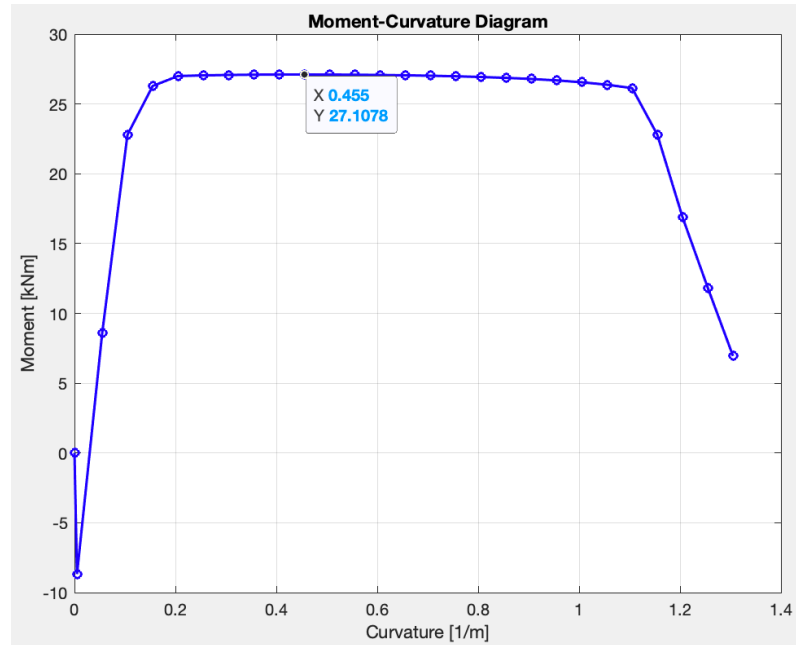


Figure 72 Output from the designed algorithm; moment-curvature diagram

The temperature profile of the structure at defined time for the 500°C isotherm method shows Figure 73.

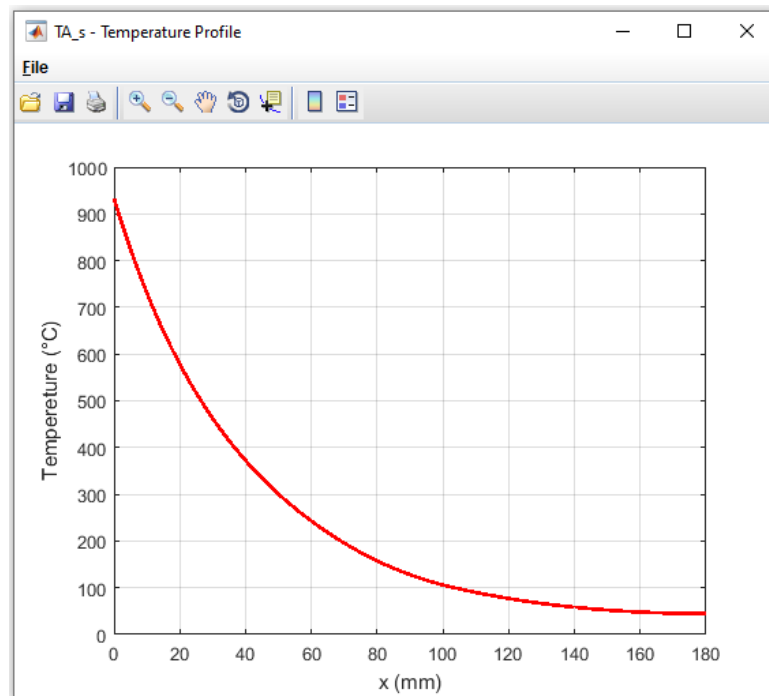


Figure 73 Temperature profile at t = 75 min (generated from [17])

In the temperature profile it can be observed that the temperature of 500°C is reached at $a_{500} = 27$ mm. The temperature in the center of reinforcing rebars at $a = 29$ mm is $\theta = 470$ °C. The 500°C isotherm method is shown in Table 2.

Table 2 Calculation with use of 500°C isotherm method

	h	=	180	mm		
	a_{500}	=	27	mm		
	h_{fi}	=	$h - a_{500}$	=	153	mm
reinforcement	θ_s	=	470	°C		
	$f_{syd,fi}$	=	$k_{s,fi} f_{yk}$	=	415	MPa
	$k_{s,fi}$	=	0.83			
	A_s	=	437	mm ²		
concrete	$f_{cd,fi}$	=	$f_{ck}/\gamma_{c,fi}$	=	30	MPa
	$\gamma_{c,fi}$	=	1			
	$\gamma_{s,fi}$	=	1			
	γ_M	=	1			
	x	=	$A_s f_{yd}/(0.8 b f_{cd})$	=	7.56	mm
	d	=	$h - c - \phi/2$	=	151	mm
	z	=	$d - 0.4 x$	=	147.98	mm
	$M_{Rd,fi}$	=	$A_s f_{sy,fi} z/\gamma_{s,fi}$	=	26.84	kNm

According to the 500°C isotherm method, the maximum moment capacity of the cross-section at $t = 75$ min is $M_{Rd} = 26.84$ kNm, which makes a total difference of 0.27 kNm from the moment calculated with the designed algorithm.

7.3.3 Benchmark example No. 3

Consider a reinforced concrete slab with following parameters:

$h = 210$ mm, $A_{s1} = 946$ mm², $A_{s2} = 0$ mm², $\phi_{s1} = 12$ mm, $c = 30$ mm, axial force $N = 0$ kN, concrete C20/25, $f_{yk} = 500$ MPa, $E_s = 200$ GPa

The slab is subjected to fire, which is in this case represented by the Isotherm 834 curve defined in EN 1991-1-2 [6]. $M_{Rd} = ?$ at time $t = 90$ min.

The temperatures in the structure are calculated in TempAnalysis [17]. The preprocessor of TempAnalysis [17] is shown in Figure 74.

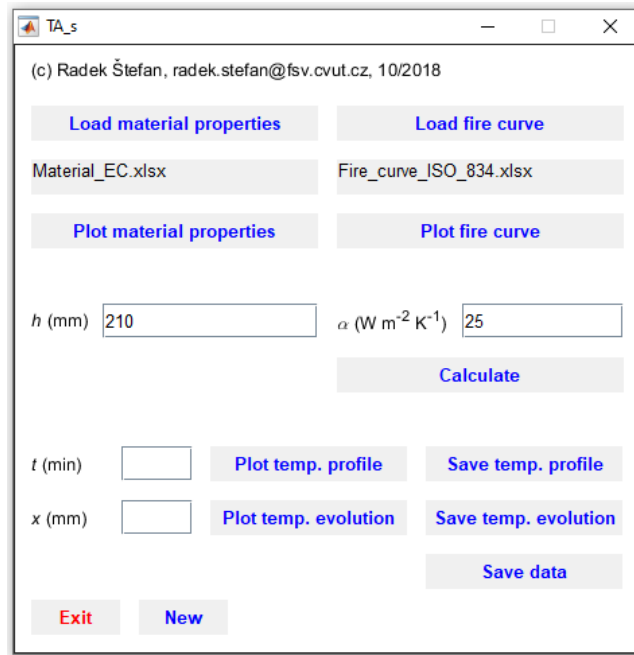


Figure 74 TempAnalysis [17] preprocessor

The input to the algorithm with the material properties and geometry is shown in Figure 75.

```

7   %input
8   -   fyk = 500; % MPa
9   -   fck = 20; % MPa
10  -   As1 = 946; % mm2/m
11  -   As2 = 0; % mm2/m
12  -   h = 210; % mm
13  -   c = 30; % mm
14  -   diam_s1 = 8; % mm lower
15  -   diam_s2 = 0; % mm upper
16  -   Es = 200000; % MPa
17
18  -   Time = 5400; % s
    
```

Figure 75 Input in the designed algorithm

The output of the algorithm shows Figure 76. According to the calculations, the maximum moment capacity of the cross-section at $t = 90$ min is $M_{Rd} = 65.96$ kNm.

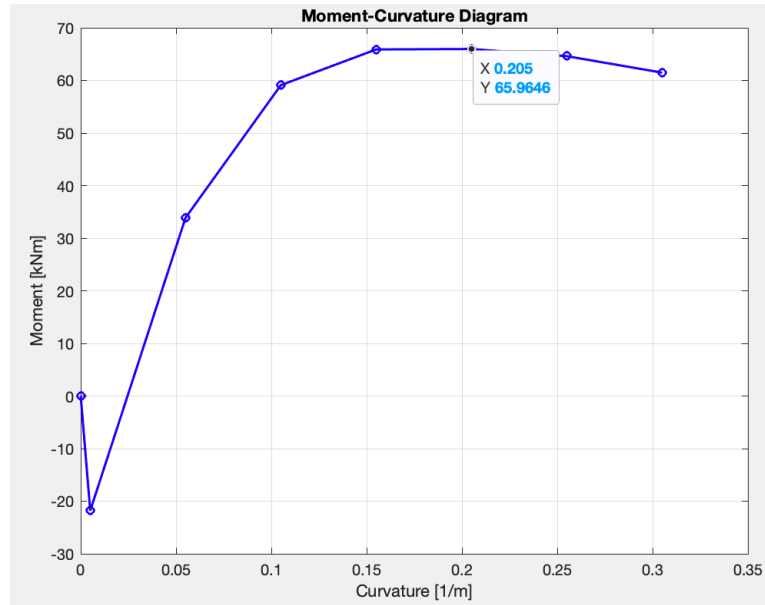


Figure 76 Output from the designed algorithm; moment-curvature diagram

The temperature profile of the structure at defined time for the 500°C isotherm method shows Figure 77.

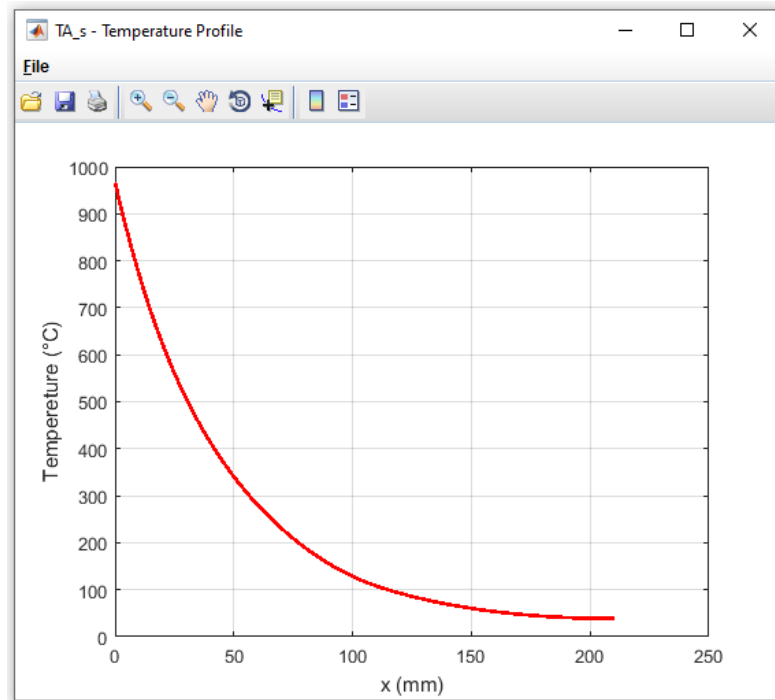


Figure 77 Temperature profile at $t = 75$ min (generated from [17])

In the temperature profile it can be observed that the temperature of 500°C is reached at $a_{500} = 30$ mm. The temperature in the center of reinforcing rebars at $a = 36$ mm is $\theta = 450^\circ\text{C}$. The 500°C isotherm method is shown in Table 3.

Table 3 Calculation with use of 500°C isotherm method

	h	=	210	mm		
	a_{500}	=	30	mm		
	h_{fi}	=	$h - a_{500}$	=	180	mm
reinforcement	θ_s	=	450	°C		
	$f_{syd,fi}$	=	$k_{s,fi} f_{yk}$	=	440	MPa
	$k_{s,fi}$	=	0.88			
	A_s	=	946	mm ²		
concrete	$f_{cd,fi}$	=	f_{cd}	=	20	MPa
	$\gamma_{s,fi}$	=	1			
	γ_M	=	1			
	x	=	$A_s f_{yd} / (0.8 b f_{cd})$	=	44.45	mm
	d	=	$h - c - \phi / 2$	=	174	mm
	z	=	$d - 0.4 x$	=	156.22	mm
	$M_{Rd,fi}$	=	$A_s f_{sy,fi} z / \gamma_{s,fi}$	=	65.03	kNm

According to the 500°C isotherm method, the maximum moment capacity of the cross-section at $t = 90$ min is $M_{Rd} = 65.03$ kNm, which makes a total difference of 0.93 kNm from the moment calculated with the designed algorithm.

7.3.4 Assessment

The differences between the moment capacity values obtained in the designed algorithm and with use of the 500°C isotherm method are in all solved benchmark examples presented in this chapter sufficiently small. The value of M_{Rd} obtained from the algorithm is in all cases slightly higher compared to the moment capacity obtained with use of the 500°C isotherm method. Since the 500°C isotherm method is a simplified procedure, it is less accurate and therefore much more conservative than a more detailed calculation which the algorithm provides, and that is why this pattern was expected and is correct.

To sum it up, based on the benchmark examples, it can be said that the algorithm works properly with a minimum error.

8 Conclusion

In this thesis, numerical methods for investigating the mechanical and thermal behavior of various structures were presented. The main focus was on creating a complex algorithm which would analyze a reinforced concrete ceiling slab exposed to thermal loading. The procedure used in the algorithm has its basis in the moment-curvature approach. The program executing the algorithm was coded in MATLAB [18].

Firstly, the moment-curvature approach was implemented for a normal temperature situation and verified with computer programs RCC [19] and InDion [20].

Then the algorithm was modified to cover the subsection of the slab to high temperatures. The procedure was then verified with the 500°C isotherm method, which is described in EN 1992-1-2 [7].

The applicability of the algorithm was proven through a series of benchmark examples, which show that the procedure provides results with sufficient accuracy.

The main contribution of this work is a design of an algorithm which analyzes reinforced concrete slabs with various material properties and geometry at normal and high temperatures.

In the future, this work can be expanded to cover not only slabs but also beams of various shapes. Moreover, a non-zero axial force can be added to the procedure which allows an extension of the applicability on different structural elements, such as columns or walls.

Literature

- [1] S. Serega, A. Wosatko. *Numerical prediction of fire resistance of RC beams*. AIP Conference Proceedings 1922, 130001 (2018). DOI 10.1063/1.5019131. <https://doi.org/10.1063/1.5019131>.
- [2] R. Štefan, J. Sura, J. Procházka, A. Kohoutková, F. Wald. *Numerical investigation of slender reinforced concrete and steel-concrete composite columns at normal and high temperatures using sectional analysis and moment-curvature approach*, Engineering Structures 190 (2019) 285–305.
- [3] J. Sura, R. Štefan, J. Procházka. *Analýza štíhlých železobetonových sloupů metodou založenou na jmenovité křivosti*, Stavební obzor 10 (2012) 294–298.
- [4] O. C. Zienkiewicz, R. L. Taylor, J. Z., Zhu. *The Finite Element Method: Its Basis and Fundamentals*. 6th ed. Oxford: Elsevier Butterworth-Heinemann, 2005. ISBN 9780080472775.
- [5] J. Holan. *Statická nelineární analýza železobetonových konstrukcí vystavených vysokým teplotám se zohledněním nejistot vstupních parametrů*. Prague, 2019. Odborná studie k rozpravě k disertační práci. CTU in Prague.
- [6] EN 1991-1-2, Eurocode 1: Actions on structures – Part 1-2: General actions – Actions on structures exposed to fire, CEN, 2002.
- [7] EN 1992-1-2, Eurocode 2: Design of concrete structures – Part 1-2: General rules –Structural fire design, CEN, 2004.
- [8] R. Štefan. Presentations for course 133PSBZ, CTU in Prague, (2012-2016). <http://people.fsv.cvut.cz/~stefarad/vyuka/133PSBZ.html>.
- [9] Module 4 Analysis of Statically Indeterminate Structures by the Direct Stiffness Method, Version 2 CE IIT, Kharagpur, *Lesson 24, The Direct Stiffness Method: Truss Analysis*.
- [10] N.-H. Kim. *Introduction to Nonlinear Finite Element Analysis*. New York: Springer US, 2015. ISBN 978-1-4419-1746-1.
- [11] J. Zeman. *Pomucka1*, Presentation for course 132MK10, CTU in Prague. <http://ksm.fsv.cvut.cz/~zemanj/teaching/mk10/cviceni/pomucka1.pdf>.
- [12] Module 4 Analysis of Statically Indeterminate Structures by the Direct Stiffness Method, Version 2 CE IIT, *Lesson 26, The Direct Stiffness Method: Temperature Changes and Fabrication Errors in Truss Analysis*.
- [13] J. Sura. *Analýza štíhlých betonových prvků vystavených extrémnímu teplotnímu namáhání*. Prague, 2018. Disertační práce. CTU in Prague.

- [14] M. Benýšek, R. Štefan, J. Procházka. *Analysis of Fire Resistance of Concrete Structural Members Based on Different Fire Models: An Illustrative Example of the Slab Panel Assessment*, Solid State Phenomena 292 (2019) 173–182.
- [15] EN 1992-1-1, Eurocode 2: Design of concrete structures – Part 1-1: General rules and rules for buildings, CEN, 2004.
- [16] M. Gelien. *Ein Beitrag zur Bemessung von Stahlbetonstützen im Brandfall*. Wuppertal, 2011. ISBN ISBN 978-3-940795-18-2. Disertační práce. Begischen Universität Wuppertal.

Software

- [17] R. Štefan, J. Procházka. *TempAnalysis – Computer program based on Finite Element Method for temperature analysis of a cross-section exposed to fire, version 1.2* [Software], CTU in Prague. <http://people.fsv.cvut.cz/~stefarad/software/ta/ta.cz.html> (2009-2016).
- [18] The MathWorks, Inc. *MATLAB, version 9.9 (R2020b)* [Software], Natick, Massachusetts, United States (2015).
- [19] J. Sura, R. Štefan, J. Procházka. *RCC – Computer program for design of reinforced concrete columns* [Software], CTU in Prague. <http://people.fsv.cvut.cz/www/stefarad/software/rcc/rcc.en.html> (2012).
- [20] J. Holan, R. Štefan. *InDion - Interaction Diagram Online* [Software], CTU in Prague. <https://people.fsv.cvut.cz/~holanjak/software/indion/program/> (2019).